Titan at the edge: 1. Titan's interaction with Saturn's magnetosphere in the prenoon sector

D. Snowden,[1] R. Winglee,[2] and A. Kidder[2]

Received 3 January 2011; revised 16 April 2011; accepted 23 May 2011; published 31 August 2011.

[1] The characteristics of Titan's environment at 09:00 Saturn local time (SLT) are studied using a three-dimensional multifluid/multiscale model of Titan embedded in a global model of Saturn's magnetosphere for three cases: a stationary magnetopause, an inward moving magnetopause, and an outward moving magnetopause. The results show that the plasma and magnetic field upstream of Titan are variable and that the variability can be enhanced when Saturn's magnetopause is not stationary. Rotating cold, interchange fingers cause rapid changes in the plasma velocity, density, and composition, while gradual changes are due to the relatively slow compression and expansion of Saturn's magnetopause. Titan enters a boundary layer on the inside of Saturn's magnetopause when Saturn's magnetopause compresses. The boundary layer is characterized by shearing flows and a mix of magnetospheric and magnetosheath plasma. The irregular flows in the boundary layer strongly modify Titan's induced magnetosphere. The results indicate that more ions from Titan are lost from Saturn's magnetosphere during parallel interplanetary magnetic field (IMF) than antiparallel IMF. In addition, we find that Titan's ion tail may be able to prevent the magnetopause from crossing Titan when Titan is in the prenoon sector. Therefore, despite a large increase in solar wind pressure, Titan remained inside of Saturn's magnetosphere. A synthetic trajectory through the simulation is shown to be consistent with magnetometer data from the TA flyby.

Citation: Snowden, D., R. Winglee, and A. Kidder (2011), Titan at the edge: 1. Titan's interaction with Saturn's magnetosphere in the prenoon sector, *J. Geophys. Res.*, *116*, A08229, doi:10.1029/2011JA016435.

1. Introduction

[2] Titan has no internal magnetic field; therefore, its atmosphere interacts directly with plasma and electromagnetic fields in Saturn's magnetosphere or, in rare cases, with the solar wind and interplanetary magnetic field (IMF). Titan's interaction with its space environment affects the chemistry, dynamics and evolution of Titan's atmosphere. The density and composition of magnetospheric plasma and the direction of Saturn's magnetic field fluctuate at Titan's orbital radius (20.3 Saturn radii, 1 R_S = 60,268 km), which is near the Saturn's dayside magnetopause [*Bertucci et al.*, 2008, 2009; *Rymer et al.*, 2009]. This region of Saturn's magnetosphere is variable because it is sensitive to both changes in the solar wind and the interplanetary magnetic field (IMF) and to internal mass loading and rotationally driven plasma exchange processes.

[3] Solar wind pressure influences Titan's magnetospheric environment by forcing Saturn's plasma disk into a bowl shape due to Saturn's high obliquity (~26.7°) and nearly aligned rotational and magnetic axis [*Arridge et al.*, 2008b]. Cassini arrived at Saturn about two years after Saturn's northern winter solstice and Saturn's spring equinox occurred in August of 2009. Therefore, during most of Cassini's prime and equinox missions the solar wind has been exerting a northward force, pushing Saturn's central current sheet above Titan's orbital plane. The hinging of the plasma sheet is strongest beyond ~15 R_S and a day-night asymmetry is apparent [*Arridge et al.*, 2008b; *Sergis et al.*, 2009]. On the night side of Saturn's magnetosphere, the hinging angle of the central current sheet is ~10° and, on the dayside, the plasma sheet is closer to the orbital plane and thicker [*Sergis et al.*, 2009].

[4] Internal plasma sources can also modify Saturn's magnetosphere near Titan. Saturn's plasma disk is mostly composed of heavy ions (~16 amu) originating from Enceladus' plume [*Hansen et al.*, 2006]. These heavy ions exert an outward centrifugal force because they are accelerated by Saturn's magnetic field, which rotates with a period of ~10.5 h. The centrifugal forcing radially stretches Saturn's magnetic field lines, giving Saturn's magnetosphere a magnetodisk structure similar to Jupiter's magnetosphere. As a result, Saturn's magnetosphere is much more compressible than Earth's magnetosphere [*Arridge et al.*, 2008b].

[1]Lunar and Planetary Laboratory, University of Arizona, Tucson, Arizona, USA.
[2]Department of Earth and Space Science, University of Washington, Seattle, Washington, USA.

0148-0227/11/2011JA016435

[5] The subsolar distances of Saturn's magnetopause observed by Cassini have a bimodal distribution with peaks at 22 and 27 R_S and range from 18 to 29 R_S [*Achilleos et al.*, 2008]. *Achilleos et al.* [2008] found that solar wind pressure variations cannot fully explain the bimodal distribution of the magnetopause distances and suggested that internal mass loading may be partially responsible. Saturn's plasma disk has been observed to extend all the way out to the magnetopause on the dayside [*Krupp et al.*, 2005], so it is feasible that the plasma disk is a main driver of magnetopause location. More recently *Kanani et al.* [2010] developed a dynamic pressure model to simulate the location of Saturn's magnetopause and found that total pressure inside Saturn's magnetosphere showed evidence of a bimodal distribution, further indicating that the bimodal distribution of Saturn's magnetopause distance is due changes within Saturn's magnetosphere rather than changes in solar wind pressure.

[6] Cassini observations of the morphology of Saturn's magnetosphere during its prime mission can be used to describe Titan's environment in Saturn's dayside magnetosphere. During the prime mission, Titan was typically located inside Saturn's magnetosphere below the central current sheet. Saturn's magnetic field near Titan was typically stretched into a magnetodisk structure by the centrifugal forcing of cold, heavy ions from Saturn's inner magnetosphere. Finally, Titan would have interacted with the plasma disk more often on the dayside of Saturn's magnetosphere because the plasma disk is closer to the orbital plane when the dayside magnetic field is compressed by the solar wind.

[7] However, Cassini observations have found that the properties of Titan's environment in all regions of Saturn's magnetosphere, including on the dayside, are anything but typical. Spacecraft observations on the dayside of Saturn's magnetosphere showed that the magnetic field and plasma near Titan varies strongly with space and time [*Neubauer et al.*, 2006; *Szego et al.*, 2005]. Variability in the density and magnetic field in Titan's environment has been also confirmed by recent studies of magnetic field and plasma data from more than 60 flybys of Cassini [*Bertucci et al.*, 2009; *Rymer et al.*, 2009; *Simon et al.*, 2010a, 2010b].

[8] In this paper we investigate the properties of Titan's environment at 09:00 Saturn local time (SLT) using a three-dimensional multifluid/multiscale model of Titan embedded in a global model of Saturn's magnetosphere. With this model we simulate the dynamics of Saturn's magnetosphere, examining the effect of changes in the solar wind pressure and IMF as well as the circulation of Saturn's plasma disk and the features of plasma interchange first simulated globally in a multifluid model by *Kidder et al.* [2009]. This model allows us to model the external and internal forcing of Saturn's magnetosphere while simultaneously modeling the properties of Titan's space environment using good resolution. The Saturn-Titan model has previously been used to illustrate how the properties of the solar wind, IMF, and the plasma disk strongly affect Titan's near space environment when the moon is located in Saturn's magnetotail [*Winglee et al.*, 2009]. Titan's local plasma environment, induced magnetotail, and ion tail are described for three periods: a stationary magnetopause, an inward moving magnetopause, and an outward moving magnetopause. In work by *Snowden et al.* [2011, hereinafter part 2], we present a simulation where Titan is in the postnoon sector of Saturn's magnetosphere (13:16 SLT) and crosses into Saturn's magnetosheath and then back into Saturn's magnetosphere.

2. Model

[9] Magnetohydrodynamic (MHD), multifluid models, and hybrid models have been developed to study Titan's plasma interaction. MHD models [e.g., *Ledvina and Cravens*, 1998; *Kabin et al.*, 1999; *Backes et al.*, 2005; *Ma et al.*, 2004] have been used to describe the general morphology of Titan's induced magnetosphere and to interpret spacecraft data, particularly in the ionosphere where ion-neutral collisions thermalize the plasma and reduce ion gyroradius effects. Hybrid models have confirmed that ion gyromotion affects the morphology of Titan's induced magnetosphere [e.g., *Brecht et al.*, 2000; *Sillanpää et al.*, 2006; *Simon et al.*, 2007; *Modolo and Chanteur*, 2008].

[10] Each modeling method has its advantages and disadvantages. One disadvantage of MHD models is that they assume that all ion species within the plasma have the same bulk velocity and solve only one momentum equation for all ions. This assumption reduces numerical complexity, however MHD models cannot determine the independent acceleration and outflow of individual ion species. Furthermore, single-fluid MHD models assume that the bulk ion velocity is equal to the bulk electron velocity. This assumption removes the Hall term in the electric field equation and ion gyroradius effects are not included in MHD simulations. Hybrid models solve for the gyromotion of particles and are able to include non-Maxwellian ion distributions. The disadvantage of hybrid models is they must solve for the motion of a large number of particles in each grid cell in order to obtain accurate statistics. Therefore, hybrid simulations are typically limited in size, duration, and/or resolution. Hybrid models have not yet been used to simulate the dynamics of large magnetospheres.

[11] Multifluid models such as the local Titan model of *Snowden et al.* [2007] and this model bridge a gap between MHD and hybrid numerical techniques. Multifluid models track the dynamics of individual ion fluids and an electron fluid and include the Hall and electron pressure gradient terms in the generalized Ohm's law. Therefore, multifluid models include mass dependent-asymmetric behavior. Multifluid models also have similar resolution and simulation volumes as MHD models. In this model, we simulate a volume of 400 × 400 × 400 R_S (400 R_S ~ 9362 R_T, 1 R_T = 2575 km) and the highest resolution near Titan is 927 km. However, multifluid models cannot simulate non-Maxwellian particle distribution and therefore currently do not include suprathermal ion and electrons populations, which may be important in Saturn's outer magnetosphere [*Kanani et al.*, 2010].

[12] To accurately study the coupled interaction between Saturn's magnetosphere and Titan it is necessary to track multiple ion populations and to include appropriately high resolution in the inner magnetosphere and near Titan. Toward this goal *Winglee et al.* [2009] developed a multifluid/multiscale model of the Saturn-Titan system, in which a local Titan model is coupled to a global Saturn model. The multifluid aspect of the model includes the dynamics from

solar wind protons, Saturn's ionospheric plasma, ions from Enceladus' plume, and Titan's ionospheric plasma. The multiscale aspect allows the local Titan model to be placed within the global Saturn model, while retaining resolution of 927 km near Titan.

2.1. Multifluid Equations

[13] The dynamics of each plasma component is described by equations for mass, momentum and pressure given by:

$$\frac{\partial \rho_i}{\partial t} + \nabla \cdot \rho_i \vec{v_i} = 0, \tag{1}$$

$$\rho_i \frac{d\vec{v_i}}{dt} = en_i\left[\vec{E} + \vec{v}_i \times \vec{B}\right] - \nabla(p_i) + \rho_i \vec{g}(r), \tag{2}$$

$$\frac{\partial p_i}{\partial t} = -\gamma \nabla \cdot (p_i \vec{v_i}) + (\gamma - 1)\vec{v_i} \cdot \nabla p_i, \tag{3}$$

where the subscript i denotes the ion components, ρ is the mass density $\vec{v}$ is the velocity, p is pressure, n is number density, e is charge, $\vec{g}$ is gravity, $\vec{B}$ and $\vec{E}$ are the magnetic and electric field. The thermal pressure is assumed to be scalar and γ is assumed to be 5/3. The electrons are assumed to have sufficiently high mobility along the field lines that they are approximately in steady state (i.e. $\frac{dv_e}{dt} = 0$), or in drift motion. This assumption removes high frequency plasma and electron waves, and enables the momentum equation for the electrons to be reduced to:

$$\vec{E} + \vec{v}_e \times \vec{B} - \frac{\nabla(p_e)}{en_e} = 0. \tag{4}$$

[14] Assuming quasi-neutrality ($n_e = \Sigma_i n_i$) and applying the definition of current ($\vec{J} = \frac{1}{\mu_0}\nabla \times \vec{B}$) the electron velocity for a multi-ion plasma becomes:

$$\vec{v_e} = \sum_i \frac{n_i}{n_e}\vec{v}_i - \frac{\vec{J}}{en_e}. \tag{5}$$

[15] Substituting equation (5) into equation (4) we find the modified Ohm's law:

$$\vec{E} = -\sum_i \frac{n_i}{n_e}\vec{v}_i \times \vec{B} + \frac{\vec{J} \times \vec{B}}{en_e} - \frac{1}{en_e}\nabla p_e + \eta \vec{J}. \tag{6}$$

Finally, the electron pressure equation is:

$$\frac{\partial p_e}{\partial t} = \gamma \nabla \cdot (p_e \vec{v_e}) + (\gamma - 1)\vec{v_e} \cdot \nabla p_e. \tag{7}$$

[16] Faraday's Law is used to close the set of equations:

$$\frac{\partial \vec{B}}{\partial t} = -\nabla \times \vec{E}. \tag{8}$$

[17] Ion cyclotron effects are included in multifluid simulations because the ion and electron species are modeled as separate fluids allowing the Hall term to be retained in Ohm's law (6). The inclusion of the Hall term implies that ions drift due to gradients in the electromagnetic fields on the order of the ion inertial scale: $L < c/\omega_{pi}$ where $\omega_{pi} = 4\pi n_i e^2/m_i$. To illustrate this, substitute the generalized Ohm's law (6) into the ion momentum equation (2),

$$\rho_i \frac{d\vec{v}_i}{dt} = en_i\left[\vec{v}_i \times \vec{B} - \sum_i \frac{n_i}{n_e}\vec{v}_i \times \vec{B} + \frac{1}{n_i}\sum_i n_i \vec{v}_i \times \vec{B} - \frac{n_e}{n_i}\vec{v}_e \times \vec{B}\right] - \nabla(p_i + p_e). \tag{9}$$

where the resistivity and gravity terms have been dropped for simplicity. The two middle terms in the bracket are zero in single-fluid MHD because $i = 1$ and $n_i = n_e$ under the assumption of quasi-neutrality giving,

$$\rho_i \frac{d\vec{v}_i}{dt} = en_i\left[\vec{v}_i \times \vec{B} - \vec{v}_e \times \vec{B}\right] - \nabla(p_i + p_e). \tag{10}$$

[18] This equation implies that $\vec{E} = -\vec{v}_e \times \vec{B}$ and that $\rho_i \frac{d\vec{v}_i}{dt} = \vec{J} \times \vec{B} - \nabla(p)$. Here $\vec{J}$ is the induced current ($\vec{J} = \frac{1}{\mu_0}\nabla \times \vec{B}$) and the ion fluid is tied to the electron fluid, which is frozen into the magnetic field. The two middle bracketed terms in equation (9) are nonzero in multifluid models and the Hall term is preserved in Ohm's law. The Hall term decouples the motion of ions and electrons, allowing additional nonsymmetric currents to form. Multifluid simulations of ion cyclotron effects in Pluto's plasma interaction have been shown to be in good agreement with hybrid simulations [*Harnett et al.*, 2005]. A local multifluid model by *Snowden et al.* [2007] also exhibits asymmetric ion outflow due to the large ion gyroradius of pickup ions from Titan's ionosphere that is very similar to the outflow simulated with the hybrid model of *Modolo and Chanteur* [2008].

2.2. Grid System

[19] Titan and Saturn's magnetosphere are coupled using a nested grid system with good resolution both near Titan and in Saturn's inner magnetosphere. The resolution of each rectangular nested grid box is shown in Figure 1. In our cartesian coordinate system Saturn's rotational axis is in the z direction, the x axis lies in Saturn's orbital plane and points away from Saturn toward the solar direction, and the y axis completes the set. Saturn is placed at [0, 0, 0] R_S. The smallest grid around Saturn is 12.5 × 12.5 × 12.5 R_S large and has a resolution of 0.25 R_S. The largest simulation box around Saturn extends 75 R_S in the solar direction and 325 R_S in the antisolar direction so that Saturn's full magnetotail can be resolved. To save computation time a Saturn only simulation was ran for the first 48 h. In this time period the solar wind and IMF transit though the simulation over 15 times, penetrating Saturn's dipole field and forming Saturn's magnetosphere until it has reached quasi steady state. Then Titan was put into Saturn's magnetosphere along with a refinement grid, as shown in Figure 1. Titan was placed at [14.14, −14.14, 0] R_S in Saturn's second finest resolved grid box is 25 × 25 × 25 R_S large and has a resolution of 0.5 R_S. This orbital position allows us to study Titan when it is near Saturn's magnetopause in the prenoon sector. The smallest grid box is 11 × 11 × 11 R_T large and has a resolution of 927 km. The refined grid around Titan covers tens of R_S, and the resolution of Titan's grid merges smoothly into Saturn's magnetospheric grid system. The equations are solved using a second-order Runge-Kutta

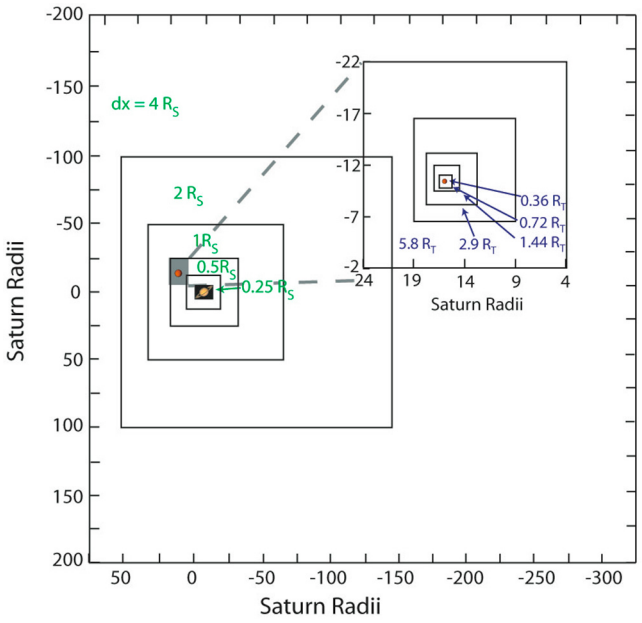

Figure 1. The grid system in the coupled Saturn-Titan model as viewed from the north and projected onto Saturn's orbital plane.

method. Plasma and field quantities are passed between grid systems at each time step, ensuring full coupling. By coupling a planetary magnetosphere with the induced magnetosphere around a moon, the multifluid/multiscale model has enabled the study of multiple plasma systems in upstream and downstream directions at small and large scales.

[20] In this simulation we have neglected the movement of Titan. We study Titan for 14 h of simulated time, during which Titan would have moved by 0.86 h of SLT. Moving this distance should not significantly change the magnetospheric conditions near Titan as Titan will still be in the predawn sector of Saturn's magnetosphere. However, for longer simulations Titan's movement may be important.

2.3. Boundary Conditions

[21] The global Saturn model utilized here [*Kidder et al.*, 2009] was originally used to determine the effect of upstream and internal conditions on the centrifugal interchange cycle in Saturn's inner magnetosphere and the coupled Saturn-Titan model was previously used to investigate Titan's interaction in the premidnight sector of Saturn's magnetosphere [*Winglee et al.*, 2009]. The model includes three ion populations: (a) protons which originate from the solar wind and Saturn's and Titan's ionosphere, (b) moderately heavy ions such as O^+, N^+, W^+ or CH_4^+ (with an assumed overall mass of 16 amu), hereafter referred to as the O^+ group and (c) heavy ions such as N_2^+ and O_2^+ (with an assumed mass of 32 amu), hereafter referred to as the heavy ion group (Hvy^+). The dynamics of the ion fluids are determined by equations (1), (2), and (3). The model also includes one electron fluid whose dynamics are determined by equations (5), (7), and (6).

[22] The presence of ions from Enceladus is incorporated into the Saturn model by placing an ion torus of O^+ with a density of 2 cm^{-3} at Enceladus' orbit (4 ± 0.5 R_S). This is consistent with early observations by Cassini [*Young et al.*, 2005]. Subsequent observations have shown that the density of Enceladus's ion torus is an order of magnitude greater [*Gurnett et al.*, 2007]. Never the less, in section 3.1, we show that the density of heavy ions simulated in Saturn's outer magnetosphere is consistent with Cassini data. Heavy ions are also initialized in this region with a density of 0.25 cm^{-3} so that Saturn's plasma disk is mostly composed of O^+ with a smaller component of Hvy^+ (28 amu) ions. The ion temperature is initialized to be cold at 18 eV, however the torus ions are rapidly heated to several hundred eV by the convection of magnetic field through the system. Where the torus comes into contact with the inner boundary of the simulation, which is placed at 2.5 R_S, the density and temperature are held constant and reset after each time step in the simulation. Saturn's magnetic field is included as a dipole with a southward polarity and a equatorial field strength of 21,000 nT at the inner boundary. The magnetic axis is aligned with the rotational axis and the rotation rate of Saturn's magnetic field is set to 10.5 h. Saturn's ionosphere, assumed to be predominantly H^+, is placed at an inner boundary of 2.25 R_S. The density of Saturn's ionosphere is assumed to be 50 cm^{-3}. The temperature of Saturn's ionospheric plasma at the inner boundary is assumed to be 1 eV which is similar to estimates of plasma temperatures in Saturn's topside ionosphere based on Cassini radio occultation measurement [*Nagy et al.*, 2006]. The density and temperature of Saturn's ionospheric plasma at the inner boundary are also held constant throughout the simulation. We neglect collisional effects of neutral gas and ring dynamics which are important in Saturn's inner magnetosphere but are beyond the scope of this paper.

[23] The inner boundary of Titan is set to 1.5 R_T where the plasma is approximately collisionless. However, near the inner boundary a small resistive term is included in the electric field equation (6) to simulate the effect of ion-neutral collisions within Titan's ionosphere. At Titan's inner boundary the density of O^+/CH_4^+ and Hvy^+ ions are set to 400 cm^{-3} each and H^+ is set to a density of 200 cm^{-3} with an exponential decrease radially away from the inner boundary. This gives a total ion density of 1000 cm^{-3} at the exobase which is on the order of the density measured by Cassini [*Ågren et al.*, 2009]. In order to account for the photoionization profile the ionospheric ion density is initialized with an exponential decrease from the subsolar to the antisolar point so that the ion density at the antisolar point is about half the density at the subsolar point. The density and temperature of ions at Titan's inner boundary are held constant and reset to their initial values after each time step. The temperature of Titan's ionosphere at the inner boundary is initialized to 0.1 eV in accordance with Cassini measurements of Titan's ionosphere [*Wahlund et al.*, 2005]. The boundary conditions for Titan are similar to those used by *Snowden et al.* [2007].

[24] The solar wind and interplanetary magnetic field (IMF) are initialized at the boundary of Saturn's largest grid box in the positive x direction. In the simulation, velocity of the solar wind varies from 450 to 540 km/s and the density varies from 0.05 and 0.1 cm^{-3}. The solar wind temperature is set to 1.4 eV. The magnitude of the IMF is set to 0.03 nT and the orientation of the IMF varies from northward to southward as described in Table 1. The obliquity of Saturn's

Table 1. Summary of the Solar Wind Parameters During Each Period of the Simulation

Period	Time (h)	B_{IMF} (nT)	P_{SW} (nPa)	R_{SW} (R_S)	D_{MP} (R_S)
1	48–53	[0, 0, 0.03]	0.016	25	5
2	53–59	[0, 0, 0.03]	0.046	19–25	2–5
3	59–62	[0, 0, −0.03]	0.046	19–22	2–4

rotational and magnetic axes change seasonally, to simulate this effect the solar wind direction is incident at an upward angle of 27°.

[25] At the inner boundaries of Saturn and Titan ions are initialized with no bulk velocity. Ion outflow from each ionosphere is achieved by pressure gradients and induced electric fields associated with the convection of magnetic fields through either system. For example, the convection of Saturn's magnetic field through Titan's ionosphere causes ions above Titan's exobase to convect downstream due to the curvature ($\vec{J} \times \vec{B}$) of field lines hung up in Titan's atmosphere which results in a sheet of plasma outflowing in Titan's wake. Pressure induced escape along magnetic field lines also causes ionospheric plasma to outflow filling the lobe regions of Titan's induced magnetosphere. The plasma outflows from Titan at ~5–15 km/s, which is consistent with Cassini measurements of the mass loaded flow near Titan [*Hartle et al.*, 2006]. The thermal velocity of Saturn's ionospheric plasma leads to a small thermal polar wind, which is enhanced by the convective electric field produced by merging of Saturn's magnetic field and the IMF. The polar wind fills Saturn's magnetosphere with H^+ ions with a temperature of ~200 eV. The rotating magnetic field accelerates the O^+ and Hvy^+ ions initialized at $L = 4 \pm 0.5$ to corotational velocities and the rapidly rotating heavy ions are centrifugally forced radially outward forming a plasma disk about Saturn's magnetic equator and deforming Saturn's magnetic field into a magnetodisk shape.

3. Results and Discussion

[26] In the following sections the evolution of Titan's space environment and Titan's induced magnetosphere and ion tail is described for a series of changes in solar wind pressure and IMF direction incident on Saturn's magnetosphere, which cause the magnetopause to move inward for several hours and then outward for several hours. A summary of the solar wind conditions is given in Table 1. First we compare the simulation results to a recent survey of Cassini measurements of Saturn's magnetosphere by *Thomsen et al.* [2010] in section 3.1. In section 3.2 we describe the plasma and magnetic field characteristics upstream of Titan. In section 3.3 we compared the plasma and magnetic field properties simulated near Titan to Cassini observations. Section 3.4 illustrates how Titan's induced magnetosphere is affected by irregular flows near Saturn's magnetopause. In section 3.5 the formation (or lack there of) of a partial ion torus is examined. In section 3.6 Titan's effect on Saturn's magnetopause is discussed. Finally, in section 3.7 the simulation results are compared to magnetometer data from Cassini's TA flyby, and it is shown that the results of the simulation are consistent with Cassini magnetometer data.

3.1. Comparison Between Cassini Data and Simulated Parameters for Saturn's Magnetosphere

[27] Several reports have been published that quantify the average plasma parameters in Saturn's magnetosphere [*Thomsen et al.*, 2010; *Wilson et al.*, 2008; *Morooka et al.*, 2009]. In this section we compare the results of this simulation to *Thomsen et al.* [2010]. Figure 2 shows both the time averaged simulation parameters and the results of *Thomsen et al.* [2010]. As discussed by *Thomsen et al.* [2010], the results of this most recent survey are mostly in good agreement with the results of the survey of *Wilson et al.* [2008] and *Morooka et al.* [2009], so we will simply focus on this most recent report. In order to derive time averaged simulation results, plasma and field quantities from 3 to 20 R_S were sampled every ~15 min in the equatorial plane radially at 00:00, 06:00, 12:00, and 18:00 SLT when Titan was in the simulations (from 48 to 62 h). The mean of these samples versus radial distance are shown in Figure 2 as solid lines. In each of the plots the standard deviation from the mean is shown with error bars.

[28] Figure 2a shows the average ion densities along the equatorial plane of the three ions in the simulation (H^+, O^+, and Hvy^+) and ion densities reported by *Thomsen et al.* [2010]. The average ion densities from *Thomsen et al.* [2010] are taken from Figure 3c of that paper, which includes ion densities measured by Cassini within 5° latitude of Saturn's equatorial plane and when Cassini's ion mass spectrometer (CAPS-IMS) [*Young et al.*, 2004] was looking directly into the corotational flow direction. In Figure 2a, the average CAPS data is shown with a larger marker while the upper and lower bound of the densities observed by CAPS are shown with smaller markers connected by dotted lines. Clearly, in the inner magnetosphere there is a significant difference between the densities of the simulation and the results of *Thomsen et al.* [2010]. The density inside of ~10 R_S is about an order of magnitude too small. However, around 10 R_S the H^+ and O^+ density predicted by the simulation is well within the range observed by Cassini CAPS. By 14 R_S the O^+ density is in good agreement with the average W^+ density reported by *Thomsen et al.* [2010]. The H^+ density predicted by the simulation remains smaller than the average H^+ density in the *Thomsen et al.* [2010] survey; however, the density predicted by the simulation is within the range of values measured by Cassini starting at ~12 R_S.

[29] The bin-averaged values of the *Thomsen et al.* [2010] survey end at 16 R_S. In the next section we will show that beyond 16 R_S, near Titan, the ion density and composition simulated are in good agreement with Cassini observations. As shown in Figure 2a the simulation predicts highly variable H^+ and O^+ densities that vary between ~.005 and 0.1 cm^{-3}, which is in good agreement with the densities measured by Cassini near Titan [e.g., *Rymer et al.*, 2009].

[30] Figure 2b compares the simulated ion temperatures and the ion temperatures reported by *Thomsen et al.* [2010]. The ion temperatures predicted by the simulation are within the range of temperatures observed by Cassini except for near ~6 R_S. In both the data and the simulation the ion temperature is very cold in Saturn's inner magnetosphere, then heats up over only a few Saturn radii and flattens out in Saturn's outer magnetosphere [*Thomsen et al.*, 2010]. In the simulation the plasma temperature rises around 4 R_S and the

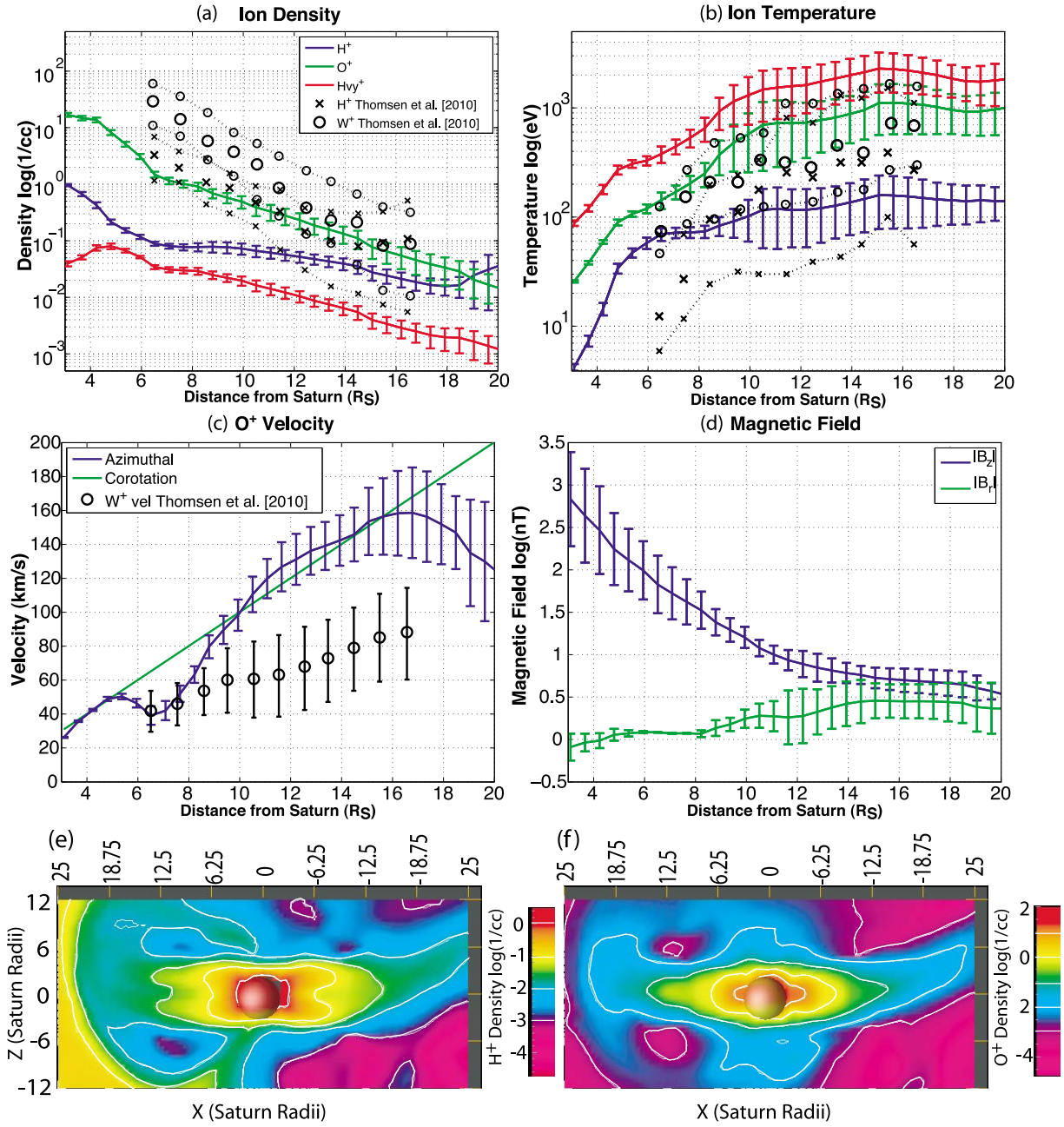

Figure 2. A comparison between model parameters and results of the survey by *Thomsen et al.* [2010]. (a) The mean H^+, O^+, and Hvy^+ density in the simulation orbital plane compared with H^+ and water group (W^+) ion densities near Saturn's equator measured by Cassini CAPS-IMS as reported by *Thomsen et al.* [2010]. The larger markers (crosses and circles) show bin-averaged data, and the smaller markers connected by dotted lines show the width of the density distribution detected by Cassini. (b) The same as Figure 2a except for ion temperature. (c) The mean azimuthal velocity O^+ plasma in the simulation's orbital plane and error bars to indicate the standard deviation from the mean, the velocity of rigid corotation, and the azimuthal velocity of water group (W^+) ions taken from *Thomsen et al.* [2010]. (d) The magnitude of the vertical (B_Z) and radial (B_r) magnetic field in the simulation's orbital plane. The simulated (e) H^+ and (f) O^+ density in the vertical plane along the Sun-Saturn axis. White lines indicate powers of 10.

ion temperature measured by CAPS appears to rise around 6 to 8 R_S. The disagreement between where the region of hotter plasma begins in the model and the data is due to difference in density, and therefore, mass loading in Saturn's inner magnetosphere described in the previous paragraph. However, similar to the density measurements the agreement between the simulation and the CAPS data is good in Saturn's outer magnetosphere.

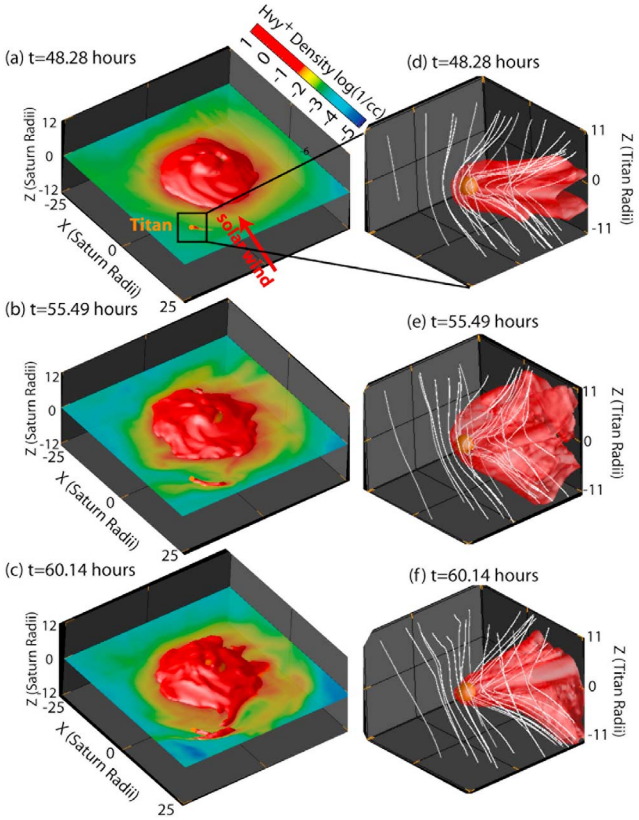

Figure 3. Two views of the Saturn-Titan simulation at three different times. (a-c) The global view of the Saturn-Titan system. The red isosurface of constant Hvy^+ density equal to 0.01 cm^{-3} and the background contour is Hvy^+ density. Titan's ionosphere and Titan's tail are imaged with the red isosurface along with heavy ions in Saturn's plasma disk. (d-f) Zoom-in of the interaction around Titan. The red surface is a surface of constant Hvy^+ density equal to 0.01 cm^{-3} showing ions outflowing from Titan, and the white lines are draped magnetic field lines.

[31] Figure 2c shows the simulated azimuthal velocity in Saturn's orbital plane along with the rigid corotation velocity and the velocity reported by *Thomsen et al.* [2010]. Deriving velocity moments from CAPS data is difficult due to the instrument's limited field of view [*Thomsen et al.*, 2010]. The velocities reported by *Thomsen et al.* [2010] are lower than the velocities reported by *Wilson et al.* [2008]. *Sittler et al.* [2006] derived plasma speeds that were much closer to, and even greater than, corotation from data taken during Cassini's orbital insertion. In any case, it appears that the average simulated velocities throughout Saturn's inner and middle magnetosphere are faster than the most recent average velocities derived from CAPS data [see also *McAndrews et al.*, 2008]. This is also due to the underestimate of the Enceladus torus density in Saturn's inner magnetosphere. Less density would result in less mass loading of plasma with 10 R_S and, therefore, faster flow velocities. In addition, a dense neutral population exist within about L = 10 R_S [*Johnson et al.*, 2006], and plasma observed by Cassini is freshly ionized cold pickup ions. Cold pickup ions attenuate momentum in Saturn's inner magnetosphere, and therefore, decrease the rotational velocity of the plasma. Including this complex neutral interaction is beyond the scope of this study. Our model predicts that the plasma flow may even become supercorotational in Saturn's middle magnetosphere. This speed up of plasma conserves momentum within the simulation, as the plasma is significantly subcorotational due to mass loading near 6.5 R_S.

[32] At radial distances greater than ~16 R_S the plasma becomes subcorotational in the simulation and the azimuthal velocity drops rapidly until it is on average about 120 km/s near Titan, which is in good agreement with estimates of plasma velocity near Titan from both Voyager and Cassini [*Hartle et al.*, 2006]. However, even if the plasma velocity near Titan is in good agreement with spacecraft measurements, the enhanced plasma velocity in Saturn's inner magnetosphere may affect how plasma is transported from Saturn's inner magnetosphere to the outer magnetosphere. Increasing the O^+ density initialized at Enceladus' torus should increase the centrifugal forcing, and therefore, radial transport of heavy plasma into Saturn's outer magnetosphere. On the other hand, increasing the plasma density also mass loads the magnetic field and reduces the rotational velocity which would decrease the centrifugal force. This should be further examined in subsequent simulations.

[33] Figure 2d shows the average vertical and radial components of Saturn's magnetic field in the orbital plane. As expected, at further orbital distances the magnetosphere is heavily affected by the centrifugal forcing of Saturn's plasma disk and the average magnitude of the radial component of the magnetic field becomes nearly half the average magnitude of the vertical component.

[34] The plasma sheet is forced into a bowl shape by the incident solar wind as described by *Arridge et al.* [2008b]. Figures 2e and 2f show the latitudinal structure of Saturn's plasma disk along the Sun-Saturn plane at 48.28 h simulated time. Figure 2e shows that the heavy plasma in Saturn's plasma disk is tightly confined to the magnetic equator. The latitudinal extend of the disk decreases with radial distances. The H^+ ions are not only more broadly distributed around Saturn's magnetic equator than O^+ but the density of H^+ peaks above and below the magnetic equator within 12 R_S. This was also seen in the diffusive model of *Persoon et al.* [2009] and *Sittler et al.* [2008]. The hydrogen ions have off-equator peaks due to an ambipolar electric field produced by the charge separation between electron and equatorially confined heavy ions, which forces the lighter H^+ off the magnetic equator.

[35] The magnetopause in Figures 2e and 2f is at ~25 R_S which is in agreement with the range of magnetopause distances measured by *Achilleos et al.* [2008] (~18 to 27 R_S). With this magnetopause distance (or at this solar wind pressure) the dayside of Saturn's magnetosphere has a magnetodisk shape which is in agreement with the results of *Arridge et al.* [2008b], who found that Saturn's dayside magnetosphere has a disk shape when the subsolar distance of the magnetopause is greater than 23 R_S and a quasi-dipolar shape when the subsolar distance of the magnetopause was less than 23 R_S. The magnetopause distance will vary throughout the simulation as we adjust the solar wind pressure however it will always be within the range observed by *Achilleos et al.* [2008].

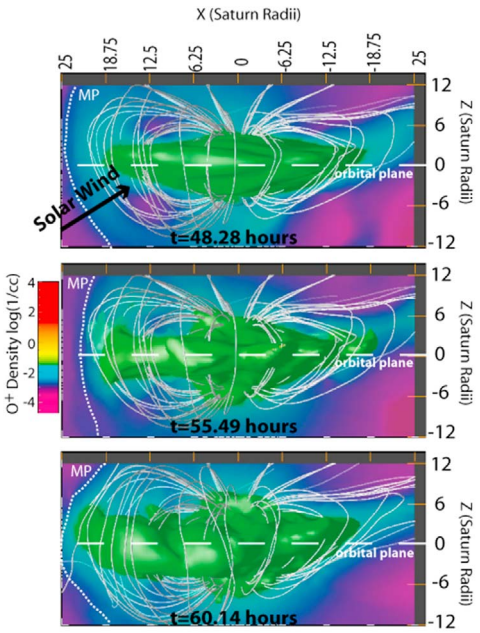

Figure 4. Saturn's plasma disk is shown with a green surface of constant O^+ density equal to 0.03 cm^{-3} and a background contour of O^+ density. The white lines show Saturn's dipole field. The short-dashed lines show the location of the magnetopause (MP). The long-dashed lines indicate Saturn's orbital plane.

[36] Although it will not be examined extensively in this paper, the overall plasma flow in the simulation is affected by both internal mass loading and the direction of the IMF. During antiparallel IMF, reconnection on the dayside transfers magnetic flux to Saturn's nightside and thins Saturn's plasma sheet similar to the Dungey cycle as shown by *Winglee et al.* [2009] and *Kidder et al.* [2009]. Periodically large amounts of heavy plasma are released down the tail in the form of plasmoids, which appears to be due to internal mass loading as described in the Vasyliunas cycle. The relative importance of Dungey-like forcing to Vasyliunas-like forcing in the Saturn simulation is the subject of a future paper.

3.2. Titan's Magnetospheric Environment During a Compression and Expansion of Saturn's Magnetopause

[37] This section describes how Saturn's magnetosphere and Titan's magnetospheric environment changes when Saturn's magnetopause compresses and expands. The description of the simulation is split into three periods: stationary magnetopause, inward moving magnetopause, and outward moving magnetopause.

3.2.1. Stationary Magnetopause

[38] As indicated in Table 1, Saturn's magnetopause is stationary (~5 R_S from Titan) for 5 h after Titan is placed in the simulation. The initial configuration of Saturn's magnetosphere and Titan's induced magnetosphere is shown in Figures 3a and 3d. Figure 3a shows Saturn's magnetosphere from above. The color contour shows the Hvy^+ density in Saturn's orbital plane and the red surface of constant Hvy^+ density shows the inner plasma disk and Titan's ion tail, which extends downstream from Titan. Figure 3d shows a close-up view of the interaction near Titan. Saturn's magnetic field lines (in white) drape around Titan. The red surface is a surface of constant Hvy^+ density equal to 0.01 cm^{-3} that shows the extent of Titan's ionosphere and ions outflowing downstream of Titan. Figure 4 shows the extent and location of Saturn's plasma disk. In Figure 4, a side view of Saturn's magnetosphere is shown from the dusk direction. The green surface is a surface of constant O^+ density equal to 0.03 cm^{-3}, which shows the three-dimensional extent of Saturn's plasma disk. Saturn's magnetic field lines are shown in white and the magnetopause and orbital plane are indicated with dashed lines. At 48.28 h, Saturn's plasma disk has a bowl shape due to the incident angle of the solar wind.

[39] We use plasma and magnetic field quantities upstream of Titan to quantify how Titan's space environment changes over time. Figure 5 shows the plasma and magnetic field characteristics at a point 20 R_T upstream of Titan. Figure 5a shows the magnetic field in Titan-centered (TIIS) coordinates. In TIIS coordinates, the x axis points in the direction of corotation, the y axis is directed from Titan toward Saturn, and the z axis points upward perpendicular to the orbital plane. Figure 5b shows the stretch and sweepback angles sampled 20 R_T upstream of Titan. The stretch angle is defined as $\arctan(B_r/B_\theta)$ and the sweepback angle is defined as $\arctan(B_\phi/B_r)$, where B_r is the radial component of the magnetic field pointing away from Saturn, B_θ is in the direction of rotation, and B_ϕ is in the direction of the cross product of the θ axis and r axis. The stretch angle describes the radial stretching of the magnetic field due to the centrifugal stress of rotating plasma. A stretch angle of 0° indicates a dipolar field and a stretch angle of +/−90° degrees indicates a completely radial field. The magnitude of the sweepback angle indicates how far the magnetic field deviates from rigid rotation. A negative sweepback angle indicates a subcorotating magnetic field and a positive sweepback angle indicates a supercorotating magnetic field. Figure 5e shows the rate of Hvy^+ outflow from Titan's ionosphere which is calculated by determining the ion flux out of a $10 \times 10 \times 10$ R_T box centered on Titan.

[40] During the first 5 h, when the magnetopause is stationary, the upstream plasma and magnetic field are stable. From 48 to 53 h the magnetic field is constant with a total magnitude of ~5 nT. During this period, Titan is below the magnetic equator (as indicated by the negative B_X) and Titan is interacting with magnetic field with a significant radial component that is subcorotational, as indicated by the stretch and sweepback angles. Figure 5c shows the upstream plasma velocity. From 48 to 53 h, the flow direction is stable in the corotational direction (x direction in TIIS). Finally, the plasma density, shown in Figure 5d, is relatively constant at ~0.01 cm^{-3} with equal amounts of H^+ and O^+. During this period of the simulation ion outflow is initially low as Titan's ion tail begins to grow but eventually becomes stable around 10^{25} ion/s.

3.2.2. Inward Moving Magnetopause

[41] At 53 h of simulated time an increase in solar wind dynamic pressure begins to compress the magnetopause and Titan's plasma environment becomes more variable. The magnetopause compresses from 53 to 59 h and, at its most compressed, the subsolar point of Saturn's magnetopause is 19 R_S and Saturn's magnetopause is located less than 2 R_S from Titan. Figure 3 illustrates the changes to Titan's ion tail

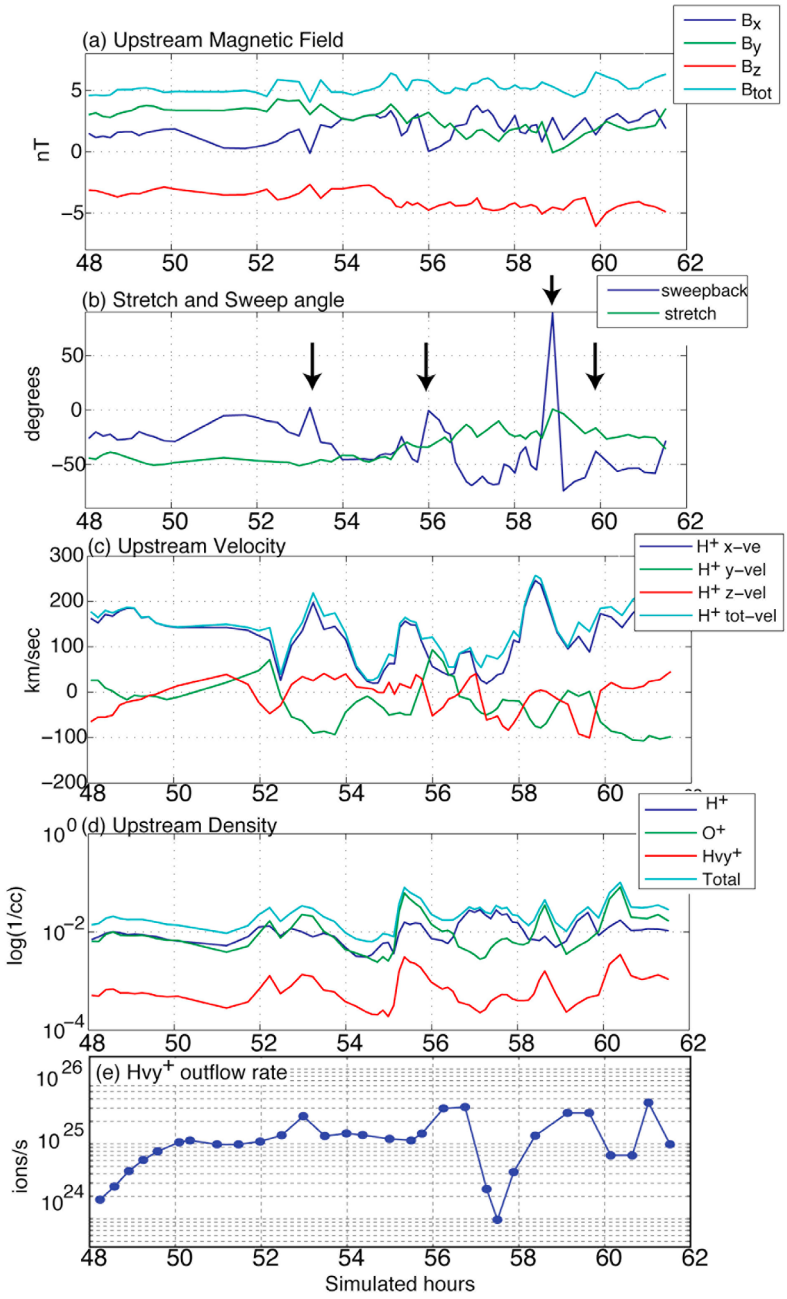

Figure 5. The simulated parameters 20 R_T upstream of Titan and the rate of Hvy^+ outflow from Titan's ionosphere. (a) The magnetic field components in TIIS coordinates, (b) sweepback and stretch angles, (c) plasma velocity, (d) ion density, and (e) Hvy^+ ion outflow from Titan's ionosphere.

and Saturn's plasma disk during the magnetopause compression. Figure 3b shows that, at 55.49 h, Titan's ion tail has grown almost reaching 12:00 SLT. Figure 3e shows ions still appear to be outflowing from Titan but the outflow region is very extended and the magnetic field is not as tightly draped as in Figure 3d. The difference in magnetic field draping and ion outflow will be further examined in section 3.4. Figure 4 shows that, at 55.49 h, Saturn's dayside plasma disk has thickened and is centered on Saturn's orbital plane. Thickening of Saturn's plasma disk is due to the increased solar wind pressure which causes Saturn's magnetic field to be more dipolar. These results agree with the findings of *Arridge et al.* [2008a], who showed that the dayside field becomes more dipolar under high solar wind pressure when the subsolar distance of the magnetopause is less than ~23 R_S.

[42] The compression of Saturn's dayside magnetosphere strongly affects Titan's space environment. The magnetic field seen in Figure 5a increases from ~5 nT to 6.5 nT. The direction of the magnetic field, initially dominated by B_Y, becomes dominated by B_Z and, as a result, the stretch angle changes from ~−50° to ~−20° on average (i.e. the field lines are more dipole like). The average sweepback angle changes from ~−20° to less than −50° which indicates an increasing

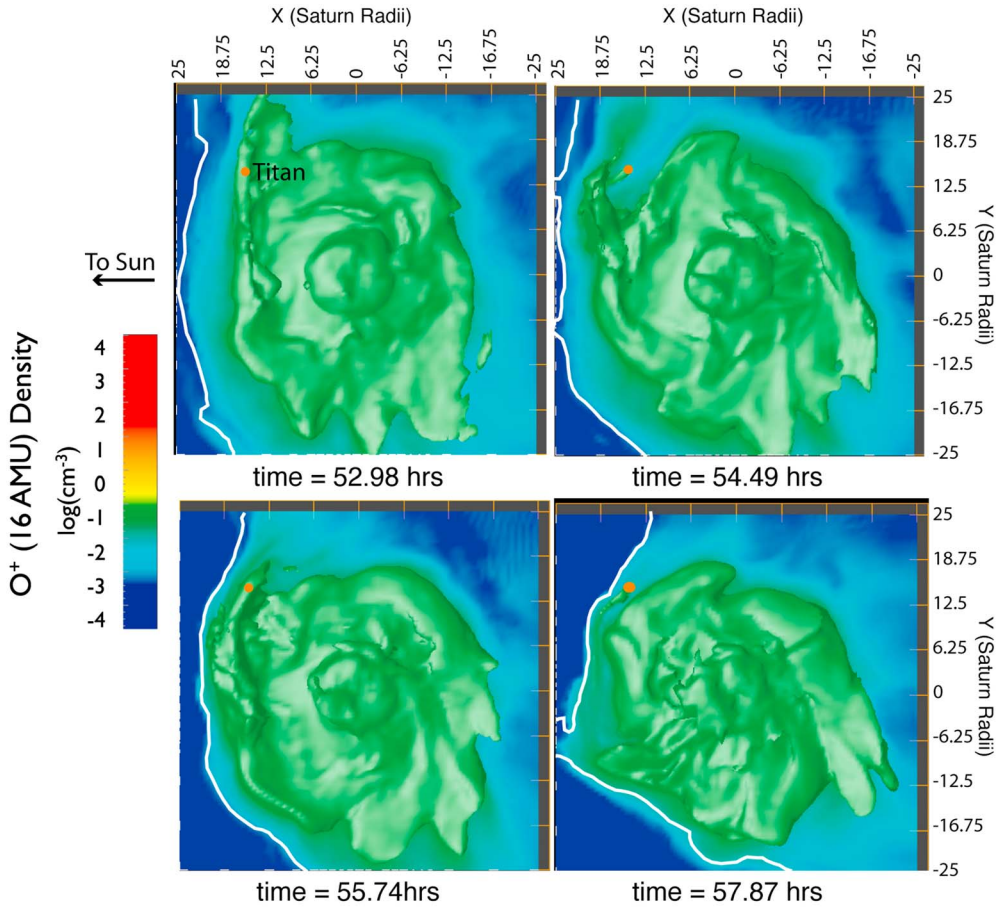

Figure 6. Saturn's plasma disk is shown from above the orbital plane with a green surface of constant O^+ density equal to 0.03 cm^{-3}. The background contour is the O^+ density in the orbital plane. The white line is the magnetopause.

departure from corotation. However, the magnitude of the sweepback angle also shows substantial decreases (indicating the flow is less subcorotational) and even turns positive (supercorotational) at times marked by arrows.

[43] The strong fluctuations in sweepback angle are correlated with sharp increases in the magnetospheric plasma flow shown in Figure 5c. The sweepback angle indicates how far the magnetic field deviates from rigid rotation and a decreasing sweepback angle indicates that the magnetic field is becoming less subcorotational. Therefore, it makes sense that the decreases in sweepback angle would be correlated with an increase in plasma velocity. The flow even becomes slightly supercorotational (positive sweepback angle) around 59 h because the plasma velocity exceeds the corotation velocity (~200 km/s). Figure 5d shows that the increases in velocity are also correlated with increases in the plasma density.

[44] The quasiperiodic behavior of Titan's upstream parameters can be explained by the rotation of finger-like regions at the edge of Saturn's plasma disk. These finger-like regions of cold plasma are caused by a large-scale interchange instability. Multifluid simulations and observations [*Burch et al.*, 2005; *André et al.*, 2005] of the interchange instability are described in detail by *Kidder et al.* [2009]. In the centrifugal interchange cycle, hot tenuous plasma sheet plasma in Saturn's outer magnetosphere moves inward, replacing cold dense ions from the Enceladus torus in Saturn's inner magnetosphere. The cooler, dense "fingers" can extend into Saturn's outer magnetosphere and have been shown to periodically interact with Titan in corresponding simulations [*Winglee et al.*, 2009]. While the interchange cycle frequently occurs during IMF that is parallel to Saturn's planetary magnetic field [*Kidder et al.*, 2009], Titan has enhanced interactions with the cold, heavy plasma fingers when the dayside magnetosphere is highly compressed, becoming more dipolar with a thickened plasma disk.

[45] Figure 6 illustrates how Titan periodically interacts with the plasma disk fingers. In Figure 6, Saturn's plasma disk is depicted by a green surface of constant O^+ density viewed from above the orbital plane. The background contour is O^+ density and the location of the magnetopause is shown with a white line. The velocity and density (shown in Figure 5) increases when a plasma disk finger sweeps past Titan. Since the fingers are not limited to Saturn's dayside magnetosphere, the strong variability in sweepback angle may be a common feature throughout Saturn's magnetosphere, which is in agreement with the variability in the

sweepback angles at all SLT reported by *Bertucci et al.* [2009].

[46] Very low and very high plasma velocities are also observed near Titan. Within the fingers the velocity is ~200 km/s and outside of the fingers the velocity is ~50 km/s. A velocity of 50 km/s is significantly slower than the average rotational speed near Titan [*Kane et al.*, 2008]. It appears that, in between Titan's interaction with the plasma disk fingers, the velocity is reduced as long as the magnetopause is moving inward (from 53 to 59 h). When the magnetopause moves inward, its motion opposes the rotational magnetospheric plasma near 09:00 SLT. Therefore, the inward compression causes a reduction in the overall plasma velocity. The plasma velocity increases inside plasma disk fingers because the centrifugal force of fingers counteracts the inward motion of the magnetopause.

[47] Figure 5e shows that the ion outflow appears to double or triple when Titan is embedded within the plasma disk fingers indicating that enhanced flow velocities near Titan lead to larger ionospheric outflows. The strong dip in ionospheric outflow near 57.75 h will be discussed in section 3.4.

3.2.3. Outward Moving Magnetopause

[48] The magnetopause begins to expand at 59 h, when the IMF turns parallel (southward), because reconnection is no longer eroding magnetic flux from Saturn's dayside magnetosphere. When the magnetopause expands, the velocity inside the tenuous regions increases, since the magnetopause is moving in the same direction as the magnetospheric plasma.

[49] In addition, the stretching angle in Figure 5b increases after the magnetopause begins to expand, indicating that the dayside of Saturn's magnetosphere is returning to a magnetodisk configuration. However, Figure 4 shows that, although the magnetopause has expanded, Saturn's plasma disk has yet to return the bowl shape seen in Figure 4 at 48.28 h. This is in agreement with Figure 5d, which shows that during the expansion period the plasma density remains fairly constant.

[50] The results indicate that the plasma and magnetic field upstream of Titan at 09:00 SLT can be quite variable when Saturn's magnetopause is not stationary. Rotating cold, interchange fingers cause rapid changes, while the more gradual changes are due to the relatively slow compression and expansion of Saturn's magnetopause.

3.3. Comparison of Simulated Parameters Upstream of Titan and Cassini Observations

[51] The simulated variability near Titan can be compared to data from Cassini's many flybys. *Rymer et al.* [2009] examined the electron density derived from Cassini's electron spectrometer (CAPS-ELS). They found that the flybys could be categorized into four different groups (plasma sheet, lobe-like, magnetosheath, or bimodal) depending on the electron energy and flux observed within 3 h of closest approach. The plasma sheet electron population identified by *Rymer et al.* [2009] had a density equal to ~0.05 cm^{-3} and the lobe electron population had electron densities equal to ~0.004 cm^{-3}. In Figure 5d, the low density regions outside of the fingers originating from Saturn's plasma disk have densities equal to 0.01 cm^{-3} or less while the regions in between these fingers have densities equal to ~0.05 to 0.1 cm^{-3}. Therefore, the rotation of Saturn's plasma disk can lead to Titan periodically being in regions where the density is lobe-like and plasma sheet-like.

[52] *Bertucci et al.* [2009] examined magnetometer data near Titan's orbit during the first 3.5 years of Cassini's mission to categorize the variability of Titan's magnetic environment. *Bertucci et al.* [2009] calculated stretch and sweepback angles from the average ambient magnetic field measured in the range $19 < \rho < 21\ R_S$ and $19 < Z < 21\ R_S$ (where ρ and Z are horizontal and vertical distances from Titan), excluding measurements in Saturn's magnetosheath or Titan's induced magnetosphere. At 09:00 SLT, the stretch angle was observed to vary from 0° to −75°. Since the stretch angle was consistently negative over the first 3.5 years of the Cassini mission, Titan's orbit appeared to be below Saturn's magnetic equator. However, Titan's orbit was at times close to the magnetic equator (as indicated by stretch angles close to 0°) and Titan was often inside of Saturn's plasma disk as indicated by *Rymer et al.* [2009].

[53] The stretch angle derived from the simulated magnetic field in Figure 5a shows similar variability from 0° to −50°. As previously, explained we find that the compression and dipolarization of Saturn's magnetic field due to the increase in solar wind pressure is responsible for the decreasing magnitude of the stretch angle. Therefore, on the dayside we find that the solar wind can have a large effect on the stretch angle, and therefore the proximity of Titan to Saturn's plasma disk. *Bertucci et al.* [2009] also found that the variation in stretch angle appeared to depend on SKR longitude, which may be due to a magnetic field anomaly (which is obviously not included in this simulation) which perturbs the field near Titan with a period of 10.7 h.

[54] *Bertucci et al.* [2009] also examined the sweepback angle near Titan and found it to be highly variable at all SLT. In the prenoon sector, the observed sweepback angle ranged from ~−50° to ~45°. The observed variation in the simulation (~−60° to ~75°) is therefore in good agreement with the Cassini observations, including the observations of supercorotating plasma indicated by positive sweepback angles. We attribute these abrupt changes in sweepback angles to the rotation of finger-like regions of plasma at the outer edges of Saturn's plasma disk.

[55] More recently, *Simon et al.* [2010a, 2010b] categorized the variability in Cassini MAG data near Titan, including all flyby's up to T62 and 79 virtual flybys or crossings of Titan's orbit with Titan not present. In particular, *Simon et al.* [2010a] noted that Saturn's plasma disk appeared to periodically flap vertically near Titan exposing Titan to plasma in Saturn's plasma sheet and causing Titan to occasionally cross Saturn's magnetic equator. *Simon et al.* [2010a] noted that the vertical motion of the current sheet appeared to occur both on short time scales and periodically on long time scales (~10.7 h). We do not simulate strong rapid vertical motion of the plasma disk and Titan never crosses the magnetic equator into the northern lobe of Saturn's magnetosphere. However, the results of our simulation are still in agreement with the findings of *Simon et al.* [2010b]. *Simon et al.* [2010b] noted that the vertical oscillations of the current sheet mostly occurred on the nightside of Saturn's magnetosphere. On the dayside, Titan was rarely

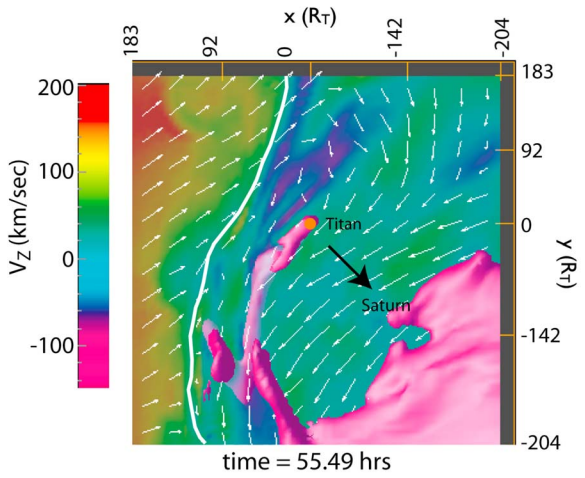

Figure 7. Plasma flow near Saturn's magnetopause. The magenta surface is a surface of constant Hvy^+ density equal to 0.01 cm^{-3} and images Titan's ion tail and part of Saturn's plasma disk. The background contour is the velocity in the z direction (in TIIS). The white line is the magnetopause. The white arrows illustrate the flow direction.

observed outside of Saturn's plasma disk. In fact, Titan was not observed in Saturn's northern lobe until around autumn equinox, when Saturn's obliquity was small and the bowl shape of Saturn's magnetodisk was relaxed.

[56] In our simulation Titan remains in Saturn's southern lobe as we are simulating conditions appropriate for southern summer. However, during our simulation the current sheet moves closer to Titan, as indicated by the stretch angle shown in Figure 5b, due to a combination of the compression of Saturn's magnetosphere by the solar wind and the rotation of Saturn's plasma disk. The dynamics simulated here likely cause the smaller scale but more frequent changes in the current sheet proximity to Titan, while large-scale periodic flapping motions are due to the magnetic anomalies associated with SKR longitude [*Bertucci et al.*, 2009; *Simon et al.*, 2010a]. An additional simulation under Saturn equinox conditions with Titan located in the magnetotail is needed to determine if the dynamics simulated by this model causes north-south oscillations of the current sheet that are large enough to cause rapid vertical motions of the current sheet across Titan.

[57] In the next section, we show how variability in Titan's space environment leads to large changes in Titan's ion tail and induced magnetosphere.

3.4. Modification of Titan's Induced Magnetosphere by Changes in Titan's Magnetospheric Environment

[58] On the inside of Saturn's magnetopause, a boundary layer exist which is analogous to the low latitude boundary layer observed in Earth's magnetosphere [*McAndrews et al.*, 2008]. Inside the boundary layer the flow direction transitions from being in a counterclockwise direction inside the magnetosphere to a clockwise direction in Saturn's magnetosheath and there is a mix of magnetosheath and magnetospheric plasma. Additionally, when the IMF is antiparallel to Saturn's planetary field, reconnection at the magnetopause accelerates plasma out of the orbital plane. Figure 7 shows the plasma flow inside the boundary later. The magenta surface is a surface of constant Hvy^+ included to illustrate the extend of Titan's ion tail. The color contour in the orbital plane shown the vertical velocity near Titan. The white line indicates the location of Saturn's magnetopause. In most of the region near Titan the vertical velocity is near zero. However, near the magnetopause there is a region where the plasma has a strong southward velocity. The white arrows show the H^+ velocity direction in the orbital plane. Near the magnetopause, upstream of Titan, the velocity rotates from being clockwise to counterclockwise. We define the boundary layer to be the region of irregular flow on the inside of Saturn's magnetosphere. The boundary layer can be wider than 2 R_S (~50 R_T) near Titan and the shearing flows in the boundary can cause Titan's ion tail to break up as seen in Figure 7.

[59] When, Titan enters the boundary layer Titan's induced magnetosphere changes drastically. Figure 8 shows the morphology of Titan's induced magnetosphere inside the boundary layer at 57.50 h and outside of the boundary layer in typical magnetospheric conditions at 61.02 h. In Figures 8a and 8b Titan's ion tail is illustrated with a magenta surface of constant Hvy^+ density. White arrows and a color contour indicate the flow velocity near Titan. In Figure 8a the plasma velocity near Titan is oriented strongly (>100 km/s) southward near the magnetopause in the boundary layer. This is in contrast to more typical plasma flow shown at a later time in 8b when Titan is further from the magnetopause. The southward plasma flow causes the morphology of Titan's induced magnetosphere to be highly irregular because, in this region, the plasma flow is no longer perpendicular to the magnetic field. Therefore, the magnetic field does not drape sharply in Titan's ionosphere because the plasma flow not carrying the magnetic field downstream. This is seen in Figures 8c and 8d, which show the Hvy^+ ion density in the orbital plane and in a vertical plane along the axis of corotation. In Figure 8c, Saturn's magnetic field lines are not draped sharply around Titan like they are in Figure 8d. Since the magnetic field lines are not curved around Titan (reducing the $\vec{J} \times \vec{B}$ force) and magnetic field lines are not moving downstream, ions do not outflow in Titan's wake. Instead, the ion density directly downstream of Titan appears patchy. This is confirmed by Figure 5e which shows that near 57.5 h ion outflow rate has dropped more than an order of magnitude to ~10^{24} ions/s. Therefore, we find that Titan's local environment and Titan's induced magnetosphere should be strongly affected by Saturn's magnetopause even if the magnetopause current sheet is several R_S away from Titan because the boundary layer inside the magnetopause is several R_S thick.

3.5. Formation and Loss of a Partial Titan Ion Torus

[60] Figure 9 shows a global view of Titan's ion tail from above Saturn' orbital plane with surface of constant Hvy^+ density and a background contour of Hvy^+ density. The magnetopause is shown with a white line. At 57.98 h Titan's ion tail has grown into a partial ion torus that extends past 12:00 SLT. However, the formation of a complete torus is interrupted when parallel IMF reaches Saturn and Saturn's magnetopause begins to expand. The outward movement of the magnetopause is seen in Figure 9 from 58.63 to 61.5 h. During this time period, large amounts of Hvy^+ ions from Titan's ion tail move across the velocity shear in the

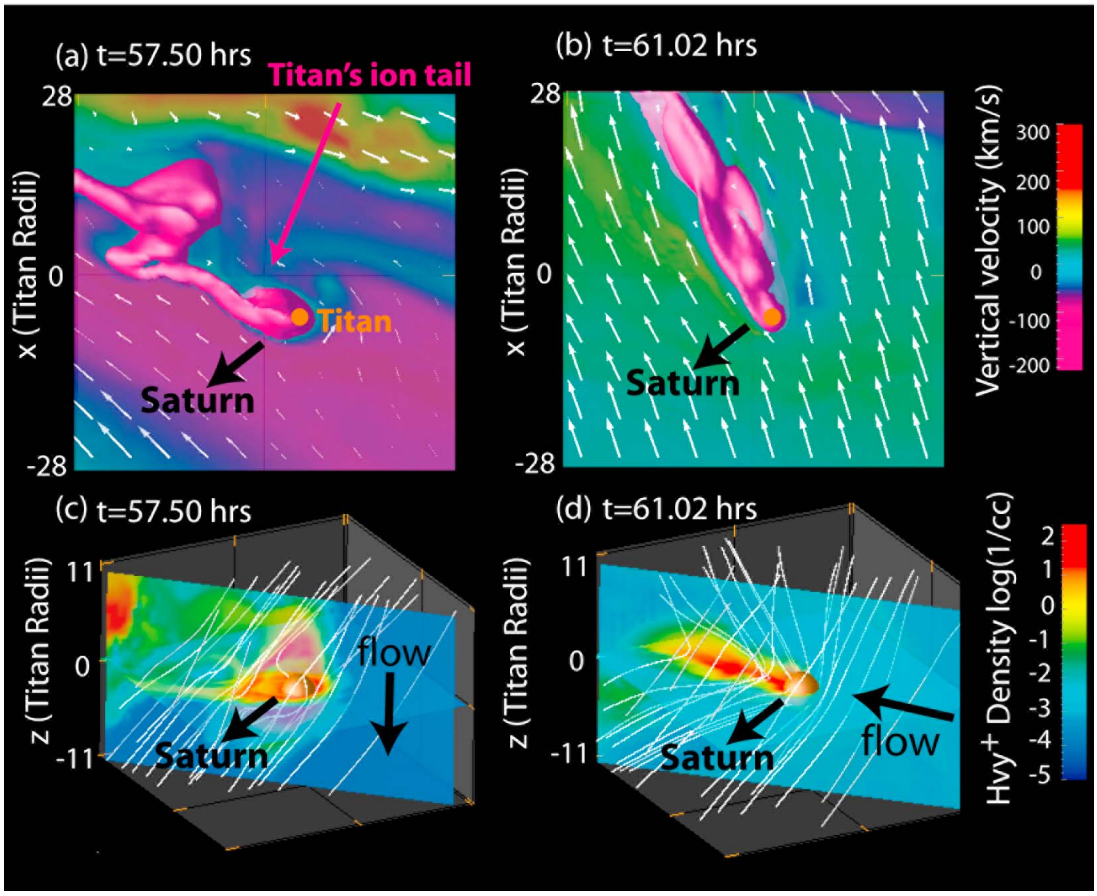

Figure 8. Two views of Titan's local environment and plasma outflow at 57.50 and 61.02 h of simulated time. (a and b) Titan's ion tail with a surface of constant Hvy^+ density and plasma velocity as in Figure 7. (c and d) Hvy^+ density in the orbital plane and along the corotation direction; the white lines are magnetic field lines.

boundary layer and flow toward Saturn's magnetotail. At the same time, ions from Titan flow along the magnetopause toward noon giving Titan's ion tail a T shape.

[61] Interestingly, more ions from Titan escape from Saturn's magnetosphere during the expansion period with parallel IMF than the compression period with antiparallel IMF despite the fact that the magnetopause is further from Titan. Heavy ions flowing along Saturn's magnetopause on the dawnside toward the tail are seen in Figure 9 only after parallel IMF reaches Saturn's magnetosphere at 59 h. The number of ions from Titan removed from Saturn's magnetosphere is difficult to quantify because ions from Saturn's plasma disk are also lost. In the future this should be remedied by separately tracking the ions from Titan and ions from Saturn's plasma disk with individual continuity equations. However, the difference in loss rates during parallel versus antiparallel IMF is evident in the growth of a long tail during antiparallel IMF and the lack of a long ion tail during parallel IMF.

[62] The simulation results indicate that less ions escape when the IMF is antiparallel because strong out-of-plane plasma velocities near the magnetopause create a barrier that prevents ions in Titan's ion tail from crossing the velocity shear. During parallel IMF the tailward flow in the boundary layer is a result of draped, southward magnetosheath field lines reconnecting with Kronian field lines at high latitudes. The reconnected magnetosheath flux tubes have the dipole shape of magnetospheric field lines, however their momentum is tailward, creating a strong shear in the plasma flow on the inside of the magnetopause. These flux tubes can mix due to instabilities (such as the Kelvin-Helmholtz), causing magnetospheric plasma to flow tailward on the dawn side of Saturn's magnetosphere. This is the primary way ions from Titan are lost during parallel IMF in our simulation.

[63] During antiparallel IMF, the situation is very different. Reconnection between magnetosheath and Kronian magnetic field occurs at low latitudes. The reconnected field lines move along the magnetopause toward the poles and the curvature force of the reconnected field lines accelerates plasma poleward parallel to the magnetopause. Figure 10 illustrates both how Titan's ion tail affects magnetopause reconnection and how reconnection affects Titan's ion tail. The color contour in Figure 10a shows H^+ ion velocity in the z direction in the orbital plane during antiparallel IMF. The regions of strong vertical plasma flow indicates that reconnection and the poleward movement of magnetic field lines is accelerating plasma near the magnetopause, which is shown with a white line. The magenta isosurface illustrates the extent of Titan's ion tail, which is deformed and

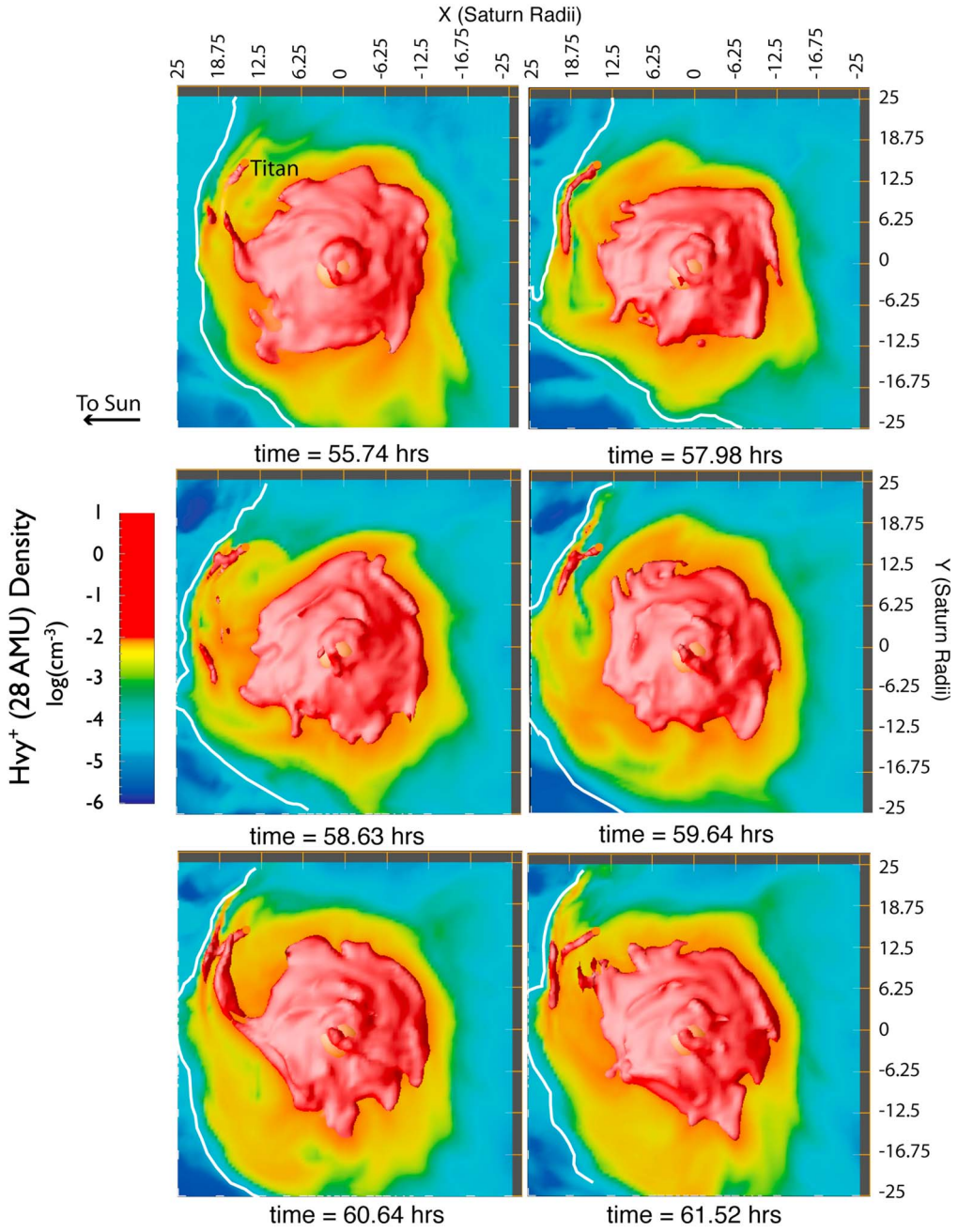

Figure 9. A global view of the growth of Titan's ion tail. The red surface is of constant Hvy^+ density equal to 0.01 cm^{-3} and images Titan's ion tail. The background contour is the Hvy^+ density in the orbital plane. The white line is the magnetopause.

extended in the vertical direction, indicating that ions in Titan's ion tail are also being accelerated out of the orbital plane by reconnection. In the simulation this is the only way ions are lost from Saturn's magnetosphere during antiparallel IMF.

[64] The deformation of Titan's ion tail can also be seen in Figure 10b. In Figure 10b, the three-dimensional, translucent yellow surface is a surface of constant velocity where v_z (H^+) = +100 km/s and is included to show that the region of strong vertical flow near Titan is bounded by U-shaped magnetic field lines (shown in red). The U-shaped magnetic field lines are recently reconnected magnetic field moving poleward. The white surfaces in Figure 10b are surfaces that show the regions where $B_{tot} < 1$ nT, indicating magnetic nulls in the model where reconnection is occurring. We find the magnetic nulls occur below Titan's orbital plane, therefore the region of southward flow near Titan is due to plasma refilling the reconnection region.

[65] Therefore, the strong vertical flows near reconnection regions may affect Titan's plasma environment. The deformation of Titan's ion tail indicates that reconnection at Saturn's magnetopause is removing ions from Titan's ion

tail. These ions may eventually end up in Saturn's auroral region or magnetotail. Their final destination is difficult to track in this simulation because Hvy^+ ions from Titan begin to mix with Hvy^+ ions from Saturn's plasma disk. In the future it would be beneficial to include individual continuity equations for ions in Saturn's magnetosphere and Titan's ionosphere. The results of the simulation would be the same but it would be possible to track the evolution and loss of plasma from Titan's ionosphere even as it mixes with plasma in Saturn's plasma disk. Although, there are no known observations of reconnection accelerating ions from Titan's ion tail, reconnection that heated and accelerated the local ion population has been observed at Saturn's dayside magnetopause [*McAndrews et al.*, 2008]. The growth of Titan's ion tail during antiparallel IMF indicates that reconnection removes ions from Saturn's magnetosphere at a much smaller rate than the tailward flow along the boundary layer that occurs during parallel IMF.

[66] Titan's ion tail may also be affecting reconnection at Saturn's magnetopause. In the simulation, the reconnection region is adjacent to Titan's ion tail but never moves radially inward of it. This is due to the heavy ions in Titan's ion tail that limit the reconnection rate by decreasing the Alfvén speed, which is shown in Figure 10c. In order for reconnection to occur, reconnected field lines must move out of the diffusion regions and fresh magnetic field lines must move into the diffusion region. The speed of the field lines is determined by the Alfvén speed, which is significantly reduced by the high density of heavy ions in Titan's ion tail. Titan's ion tail may be limiting the rate of reconnection by slowing the rate at which fresh magnetospheric field lines move into the diffusion region on the magnetospheric side and may also slow the poleward drift of reconnected field lines. Titan's affect on reconnection rates at Saturn's magnetopause may affect the magnetopause location, a topic that is discussed further in the next section.

3.6. Titan's Effect on Saturn's Magnetopause Location

[67] A primary issue that can be addressed with this simulation is how Titan affects Saturn's magnetopause distance. This question has been examined by *Wei et al.* [2009], who performed a statistical analysis of the magnetopause location measured by Cassini and determined that the magnetopause was more likely to lie inside of Titan's orbit ($<20\ R_S$) when Titan is absent from the region compared to when Titan is present.

[68] In Figures 6 and 9 the compression of Saturn's magnetopause is much stronger in the postnoon sector than in the prenoon sector. At 57.87 h the radial distance of the magnetopause is ~20 R_S at 09:00 SLT and ~17 R_S on the opposite side of noon at 15:00 SLT. This suggests that Titan's long ion tail may have some effect on the location of Saturn's magnetopause. However, asymmetry in the magnetopause could also be due to dawn-dusk asymmetries in Saturn's plasma disk and it is difficult to determine whether Titan's ion tail or Saturn's plasma disk is determining the magnetopause location.

[69] *Arridge et al.* [2008a] determined that centrifugal force from ions in the plasma disk primarily balances the dynamic pressure of the solar wind at the magnetopause. The other possible forces inside the magnetosphere, magnetic pressure and the pressure gradient force, were determined to be negligible. The results of the simulation can be used to compare the outward centrifugal forces of ions from Titan to the outward centrifugal force of Saturn's plasma disk. The centrifugal force is defined: $F = mv^2/r$, where v is the velocity of the plasma and r is the orbital radius. Titan is adding ions with a mass of ~28 amu to the plasma disk [*Wahlund et al.*, 2005]. We find that when Titan is at 09:00 SLT a partial Hvy^+ ion torus can form on Saturn's dayside with a density ~0.01 cm^{-3} near noon SLT. The density of the partial ion torus is significant compared to the ambient density in Saturn's outer magnetosphere. However, the velocity of the cold Hvy^+ ions in Titan's tail several R_S downstream of Titan is only ~50 km/s which is far less than the velocity of ions in the plasma disk. The plasma disk contains ions with masses of 16 amu that are moving with velocities of about 150 km/s. Assuming that the density of plasma sheet ions is 0.01 cm^{-3}, the centrifugal force of ions in the plasma disk is about 5 times larger than the centrifugal force of ions in Titan's ion tail. The centrifugal force of the plasma disk is even greater when suprathermal plasma pressure is included, as shown by an updated version of the model of *Arridge et al.* [2008a] by *Kanani et al.* [2010].

[70] Therefore, the plasma disk is the stronger driver of magnetopause location. As the magnetopause compresses it conforms to Saturn's plasma disk. The outer boundary of the plasma disk is highly irregular and as regions of higher density rotate to the dayside these regions determine the location and shape of the dayside magnetopause. This is evident in Figure 6 where the shape of the compressed magnetopause is seen to correlate with denser rotating regions of Saturn's plasma disk.

[71] On the other hand, the magnetopause never crosses Titan's orbit in the simulation even though, at 57.87 h, Saturn's magnetopause at 15:00 SLT is well past Titan's orbit. Therefore, it appears that Titan may be able increase the standoff distance of the magnetopause by a few R_S in its vicinity. As the magnetopause moves closer to Titan the centrifugal stress and pressure of Titan's magnetotail increases because the density of Titan's ion tail increases. The density of Titan's ion tail within a few R_S of Titan can be 0.1 cm^{-3} or more. In these regions the centrifugal force of the slow, heavy ions can exceed the centrifugal force of the plasma disk and ions from Titan can have a larger effect on magnetopause distance.

[72] Also, as described in section 3.5, Titan's ion tail may affect the location of Saturn's magnetopause in other ways. Although, Titan's tail may not have enough centrifugal forcing to push Saturn's magnetopause radially outward. Titan's ion tail may prevent (or at least slow) Saturn's magnetopause from moving inward. Titan's ion tail reduces the Alfvén speed and the reconnection rate, which could prevent the reconnection region from moving radially inward of Titan's ion tail when the IMF is antiparallel to Saturn's magnetic field.

[73] Therefore, Titan may be able to prevent itself from crossing Saturn's magnetopause by mass loading the magnetopause in its vicinity. On the prenoon side of Saturn's dayside magnetosphere, Titan's ion tail is in between Titan and the subsolar point of the magnetopause and can form a shield of heavy ions that mass load the magnetopause before it crosses Titan's orbit. However, if Titan were on the postnoon side of the magnetosphere, ions in Titan's ion tail

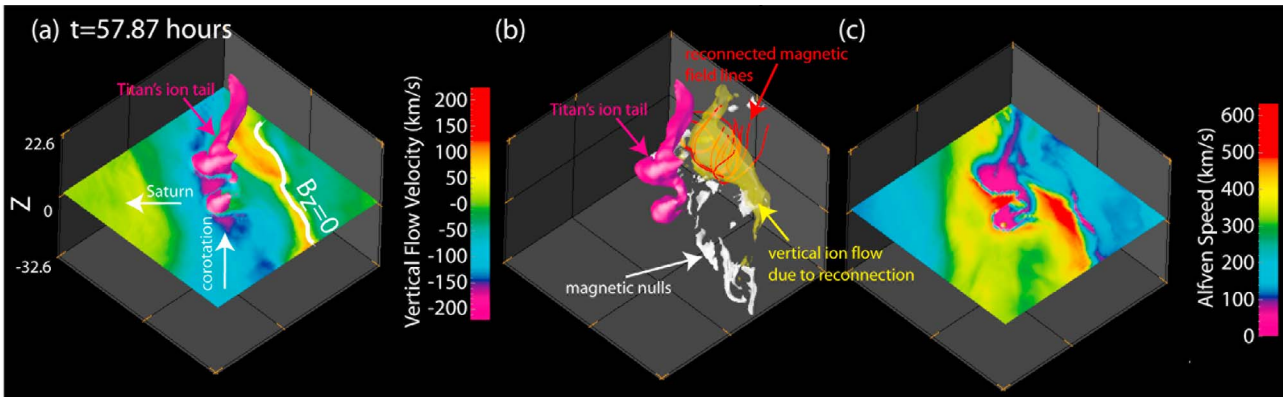

Figure 10. Three images of magnetopause reconnection near Titan and Titan's ion tail. (a) The vertical (z direction) H^+ ion velocity in the orbital plane and a surface of constant Hvy^+ density equal to 0.1 cm^{-3}, which illustrates Titan's ion tail. The white line shows the approximate location of the MP where $B_Z = 0$. (b) The magenta surface is the same as in Figure 10a, and the yellow surface shows regions where vertical velocity (V_Z) ≥ +100 km/s to indicate where plasma is accelerated by reconnection. The white surfaces show regions where the total magnetic field is <1 nT, which indicates where reconnection is occurring in the model. The red lines show recently reconnected "U"-shaped magnetic field lines. (c) The reduction in the Alfvén speed in the orbital plane due to the heavy ions in Titan's ion tail.

would not mass load the magnetopause in a way that would prevent a magnetopause crossing. This may be why the two flybys where Titan was found in the magnetosheath (T32 and T42 [e.g., *Bertucci et al.*, 2008; *Rymer et al.*, 2009]) took place in the postnoon region. In part 2, we describe a simulation with Titan at 13:16 SLT. In that simulation, Titan crosses into the magnetosheath after a similar increase in solar wind pressure.

3.7. Comparison of a Synthetic Flyby and Data From Cassini's TA Flyby

[74] There have been several Cassini flybys when Titan was in the predawn sector of Saturn's magnetosphere (e.g. TA, TB, T3, T8, and T10). In Figure 11, we compare the magnetic field results from a simulated spacecraft flown through the model in real time with data from Cassini's TA flyby and find surprisingly good agreement for such a dynamic simulation. Although the exact solar wind conditions during the encounter are unknown, the TA flyby was chosen because northward field was detected in the magnetosheath during the inbound portion of the encounter. Twelve hours of Cassini magnetometer (MAG) data [*Dougherty et al.*, 2004] are shown, which includes the TA flyby which took place at 15:30 UTC on 26 October 2004 and two magnetopause crossings which are indicated by the red lines in Figure 11. The Titan flyby occurs ~2 R_S after Cassini crossed the magnetopause [*Neubauer et al.*, 2006]. Both the Cassini MAG data and the simulated data are shown in KRTP (Saturn-centric spherical coordinates) in which B_ρ points radially away from Saturn, B_θ is the meridional coordinate and positive southward, and B_ϕ is azimuthal and positive in the direction of corotation.

[75] For comparison, the simulation data was sampled along the spacecraft trajectory starting at 48 h simulation time and 4:48 UTC time for the Cassini spacecraft. The B_θ component of the magnetic field initially starts out positive in both the simulation and in the data. The positive B_θ indicates that the spacecraft is in the magnetosphere. Next, in both the simulation results and the data, the B_θ turns negative around 8:24 UT. At this time the inward moving magnetopause has overtaken the spacecraft. The spacecraft crosses the magnetopause again on its outbound trajectory around 10:40 UTC and remains inside the magnetosphere. After traveling ~2 R_S the spacecraft encounters Titan. The spacecraft travels just downstream of Titan and inside the wake of Titan's induced magnetosphere. In Titan's wake the magnitude of the magnetic field is greatly reduced and the B_θ component is rotated into the B_ρ direction due to the draping of the magnetic field in Titan's ionosphere. The fact that the model is able to account for both the multiple magnetopause crossings made by Cassini and approximate magnetic field profiles near Titan suggests that the compression of Saturn's magnetopause to within a few R_S of Titan is indeed occurring. Briefly we will more closely examine the models prediction near Titan.

[76] The final panel in Figure 11 shows a composite ion spectrum and each ion component spectrogram for the sample satellite trajectory through the simulation. To generate the ion spectrograms a Maxwellian distribution is assumed and an energy probability distribution (based on the bulk ion temperature and velocity) is calculated at each point along the trajectory. The generation of sample spectrograms was first developed for the study of Ganymede, and the reader is referred to *Paty et al.* [2008] for a more detailed description. Unlike a CAPS ion mass spectrogram (IMS) that have a limited field of view, the sample spectrograms shows the energy and flux of ions integrated over all directions. While it is possible to artificially impose a limited field of view on our sample spectrograms to enable more precise comparisons with results from the Cassini's CAPS instrument [*Young et al.*, 2004], it would require accounting for the exact orientation of the spacecraft and sweep cycle of the instrument's actuator. This more detailed analysis would be interesting but is beyond the scope of this paper.

[77] The synthetic spectrogram can be compared to Cassini CAPS IMS data from the TA flyby described by

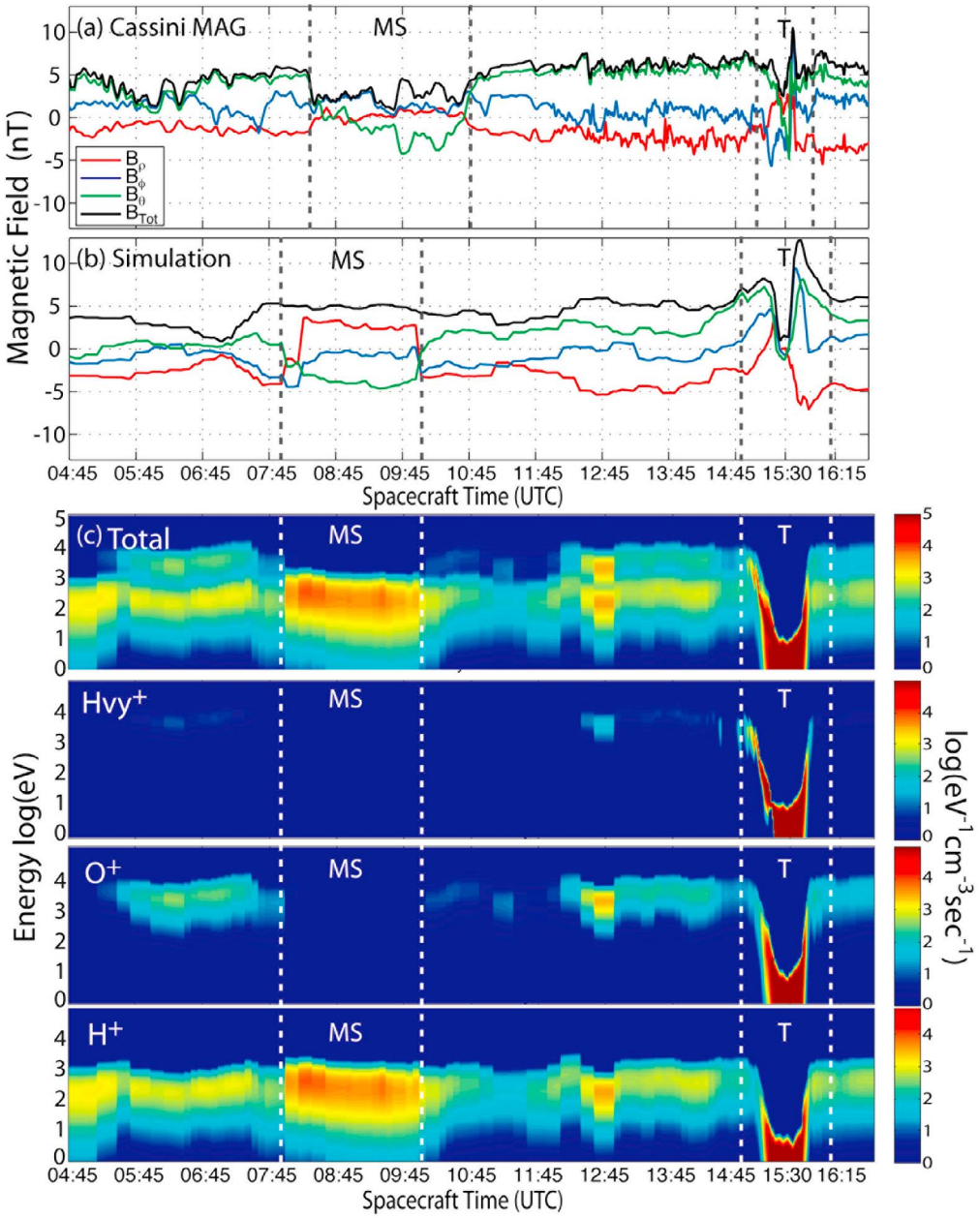

Figure 11. (a) Cassini magnetometer data from 26 October 2004 in KRTP coordinates (see text for description). (b) Magnetic field in the model in KRTP coordinates along a real-time synthetic trajectory. (c) The total and component ion spectrograms along the same synthetic spacecraft trajectory. Regions where the spacecraft is in the magnetosheath are marked with MS, and regions where the spacecraft is in Titan's mass loaded region are marked with T. At all other times the spacecraft is in Saturn's magnetosphere.

Hartle et al. [2006] and *Szego et al.* [2005]. Far from Titan, *Hartle et al.* [2006] identified two main populations in Saturn's magnetosphere. The first population was identified as H^+ and H_2^+, with an energy of ~0.016–6.3 keV for H^+. The second population was identified as O^+ with an energy ~1–4 keV. In the sample spectrogram both of these populations are apparent inside Saturn's magnetosphere. The energy of H^+ ranges from ~.02–.5 keV and the energy of O^+ ranges from ~.2–10 keV inside the magnetosphere. In the simulated spectrogram, O^+ appears quasiperiodically due to the rotation of the interchange fingers from Saturn's plasma disk. When the sample satellite is in the magnetosheath (marked with "MS") the synthetic spectrogram shows a population of relatively dense H^+ and the heavy ions are not present. When the spacecraft crosses into Titan's wake there is a large decrease in the total ion

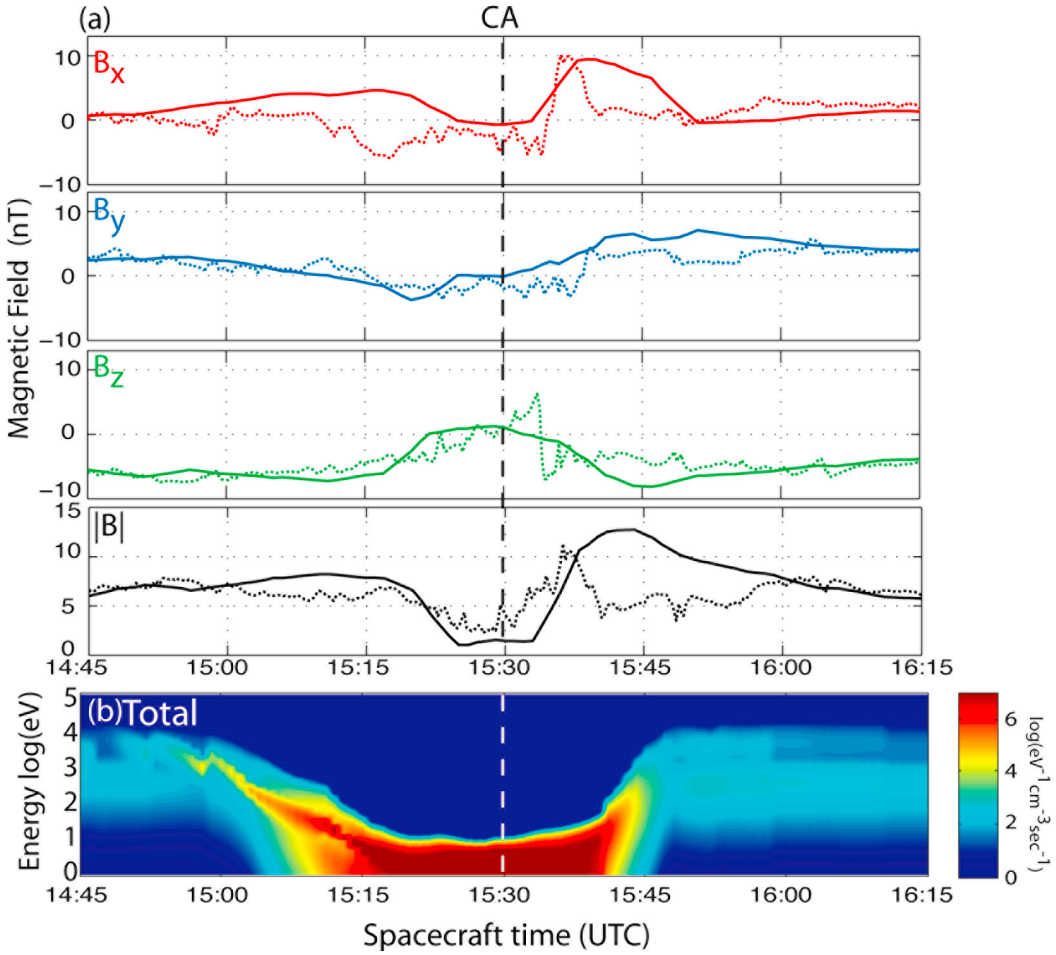

Figure 12. (a) Simulated magnetic field (solid) and magnetic field from Cassini's TA flyby (dashed). Both are shown in the TIIS coordinate system. (b) The total ion spectrograms along the same synthetic spacecraft trajectory. Cassini's closest approach (CA) at 15:30 is marked.

energy and a large increase in the density of ions, particularly Hvy^+ ions.

[78] In the CAPS data the effects of mass loading on the ambient plasma began around 15:00 UTC where ambient ion energy decreased about 3 orders of magnitude from the keV range to ~10 eV or less. In Figure 11a "T" marks the approximate mass loaded region in both the Cassini MAG data and the synthetic magnetic field data and the synthetic ion spectrograms. In the mass loaded region the magnetic field begins to rotate as Saturn's magnetic field piles up and drapes around Titan's atmosphere.

[79] *Hartle et al.* [2006] noted that the inbound and outbound deceleration of magnetospheric plasma was asymmetric in the CAPS spectrograms. The source of the asymmetry is the extended region of pickup ions on the anti-Saturn side of Titan that mass load the plasma over a larger distance. This asymmetry is also observed in the synthetic spectrogram. The decrease in energy of the ions in the spectrogram immediately before the synthetic spectrogram enters Titan's ion tail and ionosphere is more gradual on the anti-Saturn side of Titan than on the Saturn side. The asymmetry in the simulation is also caused by pickup ions on the anti-Saturn side of Titan which mass load the incident magnetic field over a larger distance. As described in section 2, asymmetric features due to ion cyclotron drifts are observed in multifluid models because the Hall term is included in the generalized Ohm's law allowing the motion of the ion fluids to decouple from the frozen-in electron fluid and undergo ion cyclotron drifts. Finally, Cassini was in Titan's ion tail and ionosphere from 15:22 to 15:40 UT, where dense low energy hydrocarbons are observed. The drop in energy from several keV to about 10 eV is also observed near that time in our synthetic spectrogram.

[80] The strong signature of H^+, O^+, and the relatively strong signature of Hvy^+ ions in the simulated spectrogram around 12:45 UTC is due to ions from Titan moving tailward inside the boundary layer (as seen in Figure 9 at 60.64 h). Therefore, despite the fact that the spacecraft is ~1 R_S from Titan in the anti-Saturnward direction and slightly upstream, heavy ions from Titan can be detected that have traveled far from Titan because of the variable flow directions in the vicinity of the boundary layer.

[81] Figure 12 shows the same data as Figure 11 but is zoomed in near Cassini's closest approach (CA) and the magnetic field data has been converted to TIIS coordinates. The predictions of this model can be compared with local

Titan models that show good agreement with MAG data with Cassini's TA flyby [*Backes et al.*, 2005; *Ma et al.*, 2006; *Modolo and Chanteur*, 2008; *Snowden et al.*, 2007]. Some features of the data are reproduced, for example the strong decrease in B_Z and the increase in B_X after CA which shows that the magnetic field is draping around Titan's ionosphere and being rotated from being primarily vertical to primarily horizontal. The B_X, B_Y, and B_Z components of Saturn's magnetic field outside of the interaction are also in good agreement. However, especially compared to the results of local models with resolution on the order of or less than 100 km [*Backes et al.*, 2005; *Ma et al.*, 2006; *Snowden et al.*, 2007] there are regions where the data and the simulations results are not in good agreement. The biggest difference is the size of the region that the magnetic field has piled up. The pileup region is much more extended after closest approach in the simulation. This may be due to the fact that the resolution of the simulation is much larger (927 km) than most local models of Titan's plasma interaction. The difference may also be due to differences in magnetospheric flow direction which would shift the orientation of draped magnetic field lines.

[82] The good agreement between the steady state models of *Backes et al.* [2005], *Ma et al.* [2006], and *Snowden et al.* [2007] indicates that, at least in the case of the TA flyby, the variability of Titan's magnetospheric environment did not have a large affect on the magnetic field in Titan's ionosphere. Even the results of our simulation do not show signatures of strong variability near Titan because closest approach takes place near 62 h of simulated time when Titan been far from the magnetopause for several hours and the plasma and flow direction are similar to what is shown in Figures 8b and 8d. However, the magnetic signature of subsequent flybys have been more difficult to explain and, in those cases, the variability of Titan's magnetospheric environment may be important.

[83] In the total ion spectrogram shown in Figure 12b the asymmetry in the deceleration of plasma inbound and out bound of the TA flyby, as described by *Hartle et al.* [2006], is apparent. In good agreement with the Cassini CAPS data described by *Hartle et al.* [2006] an extended pickup region is observed before closest approach from 15:00 UTC to 15:15 UT, the tail region is observed between 15:15 UTC and 15:45 UT. After closest approach on the Saturn facing side of Titan's ionosphere there is a much more rapid return to magnetospheric ion densities and energies which is also in agreement with the CAPS ion spectrograms of *Hartle et al.* [2006].

4. Conclusions

[84] A three-dimensional multifluid/multiscale model of Titan embedded in a global model of Saturn's magnetosphere, first described by *Winglee et al.* [2009], is used to study the characteristics of Titan's environment at 09:00 SLT. The multifluid aspect of the model allows us to include the dynamics from several ion sources and the multiscale aspect allows us to study Titan's interaction within the global Saturn model, while retaining resolution of 927 km near Titan. Therefore, we are able to determine how the dynamics of Saturn's magnetopause and plasma disk affect Titan's space environment at 09:00 SLT and how those changes affect Titan's induced magnetosphere.

[85] Titan's local plasma environment, induced magnetotail, and ion tail were described for three periods: a stationary magnetopause, an inward moving magnetopause, and an outward moving magnetopause. The results show that the plasma and magnetic field upstream of Titan are variable when Saturn's magnetopause is not stationary. Rotating cold, interchange fingers cause rapid changes in the plasma velocity, density, and composition, while the more gradual changes are due to the relatively slow compression and expansion of Saturn's magnetopause. When the magnetopause compresses Titan can enter a boundary layer on the inside of Saturn's magnetopause, which is characterized by shearing flows and a mix of magnetospheric and magnetosheath plasma. The boundary layer was shown to be several R_S thick. The irregular flow in the boundary layer is shown to strongly modify the morphology of Titan's induced magnetosphere during periods when the magnetopause is compressed and located within several R_S of Titan.

[86] Prior to Cassini's arrival, it was believed that a nitrogen ion torus might form at Titan's orbit [*Smith et al.*, 2004]. An ion torus at Titan's orbit has even been incorporated into models of Saturn's magnetosphere [*Hansen et al.*, 2005]. If such a torus existed the mass loading of the torus plasma could have a global effect on Saturn's magnetosphere. However, Cassini has not detected a nitrogen ion torus at Titan's orbit and the nitrogen ions detected in Saturn's inner magnetosphere were determined to have come from Enceladus [*Smith et al.*, 2007]. *Smith et al.* [2007] showed that Titan's ion torus should be above the detection threshold of Cassini's plasma detectors, therefore either the loss rate from Titan has been overestimated or ions from Titan are lost from Saturn's magnetosphere before they can form a into a full torus. The simulation described in this paper shows how ions from Titan may be lost from Saturn's magnetosphere. We find that more ions from Titan are lost from Saturn's magnetosphere during parallel IMF than antiparallel IMF. During antiparallel IMF, Titan's ion tail extends hundreds R_T across Saturn's dayside magnetosphere and a relatively small number of ions from Titan's may be lost from Saturn's magnetosphere due to dayside reconnection. During parallel IMF, ions originating from Titan leak across the velocity shear in the boundary layer and are lost from Saturn's magnetosphere.

[87] Another question that can be addressed with this simulation is how Titan affects Saturn's magnetopause distance. The simulation results indicate that, over most of the dayside magnetosphere, the centrifugal force of Saturn's plasma disk is greater than the centrifugal force of ions in Titan's ion tail on Saturn's magnetopause. The centrifugal forcing of the heavy ions is limited because the velocity of the heavy ions is less than the velocity of ions in the plasma disk. Therefore, the plasma disk determines the magnetopause location. However, when the magnetopause is compressed and Titan is in the prenoon sector, ions from Titan can exert a large force on the magnetopause in its vicinity and potentially prevent the magnetopause from crossing Titan's orbit. In addition, Titan's ion tail may prevent (or at least slow) the inward motion of Saturn's magnetopause when Titan is in the prenoon sector because heavy ions in

Titan's ion tail significantly reduce the Alfvén velocity and, therefore, the reconnection rate.

[88] Finally, a synthetic trajectory through the simulation is shown to be in good agreement with magnetometer data from the TA flyby, including the detection of two magnetopause crossings. The agreement between the synthetic data and Cassini data indicates that the magnetopause is very dynamic near Titan and can move within several R_S of Titan. Due to irregular flows in Saturn's dawnside boundary layer, ions originating from Titan were detected very far from (~1 R_S) and slightly upstream of Titan. This result may contribute to the analysis of Cassini ion spectra because it indicates that ions from Titan can be detected very far from Titan due to the irregular flow pattern near Saturn's dawnside magnetopause.

[89] In part 2, we present a similar simulation with Titan at 13:16 SLT. In this simulation, Titan crosses into Saturn's magnetosheath when the magnetopause is compressed by an increase in solar wind pressure. After a few hours Titan crosses back into the magnetosphere when the plasma disk pushes Saturn's magnetopause outward. We observe how the magnetopause crossing and magnetosheath environment affects the characteristics of Titan's induced magnetosphere and compare our simulation results to data from Cassini's T32 flyby.

[90] **Acknowledgments.** This work was supported by NASA grants NNX07AJ80G and NNX08AR16G and the NSF Astrobiology Program at the University of Washington.

[91] Masaki Fujimoto thanks the reviewers for their assistance in evaluating this paper.

References

Achilleos, N., C. S. Arridge, C. Bertucci, C. M. Jackman, M. K. Dougherty, K. K. Khurana, and C. T. Russell (2008), Large-scale dynamics of Saturn's magnetopause: Observations by Cassini, *J. Geophys. Res.*, *113*, A11209, doi:10.1029/2008JA013265.

Ågren, K., J.-E. Wahlund, P. Garnier, R. Modolo, J. Cui, M. Galand, and I Müller-Wodarg (2009), On the ionospheric structure of Titan, *Planet. Space Sci.*, *57*(14–15), 1821–1827, doi:10.1016/j.pss.2009.04.012.

André, N., M. K. Dougherty, C. T. Russell, J. S. Leisner, and K. K. Khurana (2005), Dynamics of the Saturnian inner magnetosphere: First inferences from the Cassini magnetometers about small-scale plasma transport in the magnetosphere, *Geophys. Res. Lett.*, *32*, L14S06, doi:10.1029/2005GL022643.

Arridge, C. S., C. T. Russell, K. K. Khurana, N. Achilleos, S. W. H. Cowley, M. K. Dougherty, D. J. Southwood, and E. J. Bunce (2008a), Saturn's magnetodisc current sheet, *J. Geophys. Res.*, *113*, A04214, doi:10.1029/2007JA012540.

Arridge, C. S., K. K. Khurana, C. T. Russell, D. J. Southwood, N. Achilleos, M. K. Dougherty, A. J. Coates, and H. K. Leinweber (2008b), Warping of Saturn's magnetospheric and magnetotail current sheets, *J. Geophys. Res.*, *113*, A08217, doi:10.1029/2007JA012963.

Backes, H., et al. (2005), Titan's magnetic field signature during the first Cassini encounter, *Science*, *308*, 992–995, doi:10.1126/science.1109763.

Bertucci, C., et al. (2008), The magnetic memory of Titan's ionized atmosphere, *Science*, *321*, 1475–1478, doi:10.1126/science.1159780.

Bertucci, C., B. Sinclair, N. Achilleos, P. Hunt, M. K. Dougherty, and C. S. Arridge (2009), The variability of Titan's magnetic environment, *Planet. Space Sci.*, *57*(14–15), 1813–1820, doi:10.1016/j.pss.2009.02.009.

Brecht, S. H., J. G. Luhmann, and D. J. Larson (2000), Simulation of the Saturnian magnetospheric interaction with Titan, *J. Geophys. Res.*, *105*(A6), 13,119–13,130, doi:10.1029/1999JA900490.

Burch, J. L., J. Goldstein, T. W. Hill, D. T. Young, F. J. Crary, A. J. Coates, N. Andre, W. S. Kurth, and E. C. Sittler Jr. (2005), Properties of local plasma injections in Saturn's magnetosphere, *Geophys. Res. Lett.*, *32*, L14S02, doi:10.1029/2005GL022611.

Dougherty, M. K., et al. (2004), The Cassini magnetic field investigation, *Space Sci. Rev.*, *114*(1), 331–383, doi:10.1007/s11214-004-1432-2.

Gurnett, D. A., A. M. Persoon, W. S. Kurth, J. B. Groene, T. F. Averkamp, M. K. Dougherty, and D. J. Southwood (2007), The variable rotation period of the inner region of Saturn's plasma disk, *Science*, *316*, 442–445, doi:10.1126/science.1138562.

Hansen, C. J., A. L. Esposito, J. Stewart, A. Colwell, A. Hendrix, W. Pryor, D. Shemansky, and R. West (2006), Enceladus' water vapor plume, *Science*, *311*, 1422–1425, doi:10.1126/science.1121254.

Hansen, K. C., A. J. Ridley, G. B. Hospodarsky, N. Achilleos, M. K. Dougherty, T. I. Gombosi, and G. Tóth (2005), Global MHD simulations of Saturn's magnetosphere at the time of Cassini approach, *Geophys. Res. Lett.*, *32*, L20S06, doi:10.1029/2005GL022835.

Harnett, E. M., R. M. Winglee, and P. A. Delamere (2005), Three-dimensional multi-fluid simulations of Pluto's magnetosphere: A comparison to 3D hybrid simulations, *Geophys. Res. Lett.*, *32*, L19104, doi:10.1029/2005GL023178.

Hartle, R. E., et al. (2006), Initial interpretation of Titan plasma interaction as observed by the Cassini plasma spectrometer: Comparisons with Voyager 1, *Planet. Space Sci.*, *54*(12), 1211–1224, doi:10.1016/j.pss.2006.05.029.

Johnson, R. E., H. T. Smith, O. J. Tucker, M. Liu, M. H. Burger, E. C. Sittler, and R. L. Tokar (2006), The Enceladus and OH tori at Saturn, *Astrophys. J.*, *644*(2), L137–L139, doi:10.1086/505750.

Kabin, K., T. I. Gombosi, D. L. De Zeeuw, K. G. Powell, and P. L. Israelevich (1999), Interaction of the Saturnian magnetosphere with Titan: Results of a three-dimensional MHD simulation, *J. Geophys. Res.*, *104*(A2), 2451–2458, doi:10.1029/1998JA900080.

Kanani, S. J., et al. (2010), A new form of Saturn's magnetopause using a dynamic pressure balance model, based on in situ, multi-instrument Cassini measurements, *J. Geophys. Res.*, *115*, A06207, doi:10.1029/2009JA014262.

Kane, M., D. G. Mitchell, J. F. Carbary, S. M. Krimigis, and F. J. Crary (2008), Plasma convection in Saturn's outer magnetosphere determined from ions detected by the Cassini INCA experiment, *Geophys. Res. Lett.*, *35*, L04102, doi:10.1029/2007GL032342.

Kidder, A., R. M. Winglee, and E. M. Harnett (2009), Regulation of the centrifugal interchange cycle in Saturn's inner magnetosphere, *J. Geophys. Res.*, *114*, A02205, doi:10.1029/2008JA013100.

Krupp, N., et al. (2005), The Saturnian plasma sheet as revealed by energetic particle measurements, *Geophys. Res. Lett.*, *32*, L20S03, doi:10.1029/2005GL022829.

Ledvina, S. A., and T. E. Cravens (1998), A three-dimensional MHD model of plasma flow around Titan, *Planet. Space Sci.*, *46*(9–10), 1175–1191, doi:10.1016/S0032-0633(98)00052-X.

Ma, Y.-J., A. F. Nagy, T. E. Cravens, I. V. Sokolov, J. Clark, and K. C. Hansen (2004), 3-D global MHD model prediction for the first close flyby of Titan by Cassini, *Geophys. Res. Lett.*, *31*, L22803, doi:10.1029/2004GL021215.

Ma, Y., A. F. Nagy, T. E. Cravens, I. V. Sokolov, K. C. Hansen, J.-E. Wahlund, F. J. Crary, A. J. Coates, and M. K. Dougherty (2006), Comparisons between MHD model calculations and observations of Cassini flybys of Titan, *J. Geophys. Res.*, *111*, A05207, doi:10.1029/2005JA011481.

McAndrews, H. J., C. J. Owen, M. F. Thomsen, B. Lavraud, A. J. Coates, M. K. Dougherty, and D. T. Young (2008), Evidence for reconnection at Saturn's magnetopause, *J. Geophys. Res.*, *113*, A04210, doi:10.1029/2007JA012581.

Modolo, R., and G. M. Chanteur (2008), A global hybrid model for Titan's interaction with the Kronian plasma: Application to the Cassini TA flyby, *J. Geophys. Res.*, *113*, A01317, doi:10.1029/2007JA012453.

Morooka, M. W., et al. (2009), The electron density of Saturn's magnetosphere, *Ann. Geophys.*, *27*, 2971–2991, doi:10.5194/angeo-27-2971-2009.

Nagy, A. F., et al. (2006), First results from the ionospheric radio occultations of Saturn by the Cassini spacecraft, *J. Geophys. Res.*, *111*, A06310, doi:10.1029/2005JA011519.

Neubauer, F. M., et al. (2006), Titan's near magnetotail from magnetic field and electron plasma observations and modeling: Cassini flybys TA, TB, and T3, *J. Geophys. Res.*, *111*, A10220, doi:10.1029/2006JA011676.

Paty, C., W. Paterson, and R. Winglee (2008), Ion energization in Ganymede's magnetosphere: Using multifluid simulations to interpret ion energy spectrograms, *J. Geophys. Res.*, *113*, A06211, doi:10.1029/2007JA012848.

Persoon, A. M., et al. (2009), A diffusive equilibrium model for the plasma density in Saturn's magnetosphere, *J. Geophys. Res.*, *114*, A04211, doi:10.1029/2008JA013912.

Rymer, A. M., H. T. Smith, A. Wellbrock, A. J. Coates, and D. T. Young (2009), Discrete classification and electron energy spectra of Titan's varied magnetospheric environment, *Geophys. Res. Lett.*, *36*, L15109, doi:10.1029/2009GL039427.

Sergis, N., S. M. Krimigis, D. G. Mitchell, D. C. Hamilton, N. Krupp, B. H. Mauk, E. C. Roelof, and M. K. Dougherty (2009), Energetic particle pressure in Saturn's magnetosphere measured with the Magnetospheric Imaging Instrument on Cassini, *J. Geophys. Res.*, *114*, A02214, doi:10.1029/2008JA013774.

Sillanpää, I., E. Kallio, P. Janhunen, W. Schmidt, K. Mursula, J. Vilppola, and P. Tanskanen (2006), Hybrid simulation study of ion escape at Titan for different orbital positions, *Adv. Space Res.*, *38*(4), 799–805, doi:10.1016/j.asr.2006.01.005.

Simon, S., A. Boesswetter, T. Bagdonat, U. Motschmann, and J. Schuele (2007), Three-dimensional multispecies hybrid simulation of Titan's highly variable plasma environment, *Ann. Geophys.*, *25*, 117–144, doi:10.5194/angeo-25-117-2007.

Simon, S., A. Wennmacher, F. M. Neubauer, C. L. Bertucci, H. Kriegel, J. Saur, C. T. Russell, and M. K. Dougherty (2010a), Titan's highly dynamic magnetic environment: A systematic survey of Cassini magnetometer observations from flybys TA-T62, *Planet. Space Sci.*, *58*(10), 1230–1251, doi:10.1016/j.pss.2010.04.021.

Simon, S., A. Wennmacher, F. M. Neubauer, C. L. Bertucci, H. Kriegel, C. T. Russell, and M. K. Dougherty (2010b), Dynamics of Saturn's magnetodisk near Titan's orbit: Comparison of Cassini magnetometer observations from real and virtual Titan flybys, *Planet. Space Sci.*, *58*(12), 1625–1635, doi:10.1016/j.pss.2010.08.006.

Sittler, E. C., et al. (2006), Cassini observations of Saturn's inner plasmasphere: Saturn orbit insertion results, *Planet. Space Sci.*, *54*(12), 1197–1210, doi:10.1016/j.pss.2006.05.038.

Sittler, E. C., Jr., et al. (2008), Ion and neutral sources and sinks within Saturn's inner magnetosphere: Cassini results, *Planet. Space Sci.*, *56*(1), 3–18, doi:10.1016/j.pss.2007.06.006.

Smith, H. T., R. E. Johnson, and V. I. Shematovich (2004), Titan's atomic and molecular nitrogen tori, *Geophys. Res. Lett.*, *31*, L16804, doi:10.1029/2004GL020580.

Smith, H. T., R. E. Johnson, E. C. Sittler, M. Shappirio, D. Reisenfeld, O. J. Tucker, M. Burger, F. Crary, D. J. McComas, and D. T. Young (2007), Enceladus: The likely dominant nitrogen source in Saturn's magnetosphere, *Icarus*, *188*(2), 356–366, doi:10.1016/j.icarus.2006.12.007.

Snowden, D., R. Winglee, C. Bertucci, and M. Dougherty (2007), Three-dimensional multifluid simulation of the plasma interaction at Titan, *J. Geophys. Res.*, *112*, A12221, doi:10.1029/2007JA012393.

Snowden, D., R. Winglee, and A. Kidder (2011), Titan at the edge: 2. A global simulation of Titan exiting and reentering Saturn's magnetosphere at 13:16 Saturn local time, *J. Geophys. Res.*, *116*, A08230, doi:10.1029/2011JA016436.

Szego, K., et al. (2005), The global plasma environment of Titan as observed by Cassini plasma spectrometer during the first two close encounters with Titan, *Geophys. Res. Lett.*, *32*, L20S05, doi:10.1029/2005GL022646.

Thomsen, M. F., D. B. Reisenfeld, D. M. Delapp, R. L. Tokar, D. T. Young, F. J. Crary, E. C. Sittler, M. A. McGraw, and J. D. Williams (2010), Survey of ion plasma parameters in Saturn's magnetosphere, *J. Geophys. Res.*, *115*, A10220, doi:10.1029/2010JA015267.

Wahlund, J.-E., et al. (2005), Cassini measurements of cold plasma in the ionosphere of Titan, *Science*, *308*, 986–989, doi:10.1126/science.1109807.

Wei, H. Y., C. T. Russell, A. Wellbrock, M. K. Dougherty, and A. J. Coates (2009), Plasma environment at Titan's orbit with Titan present and absent, *Geophys. Res. Lett.*, *36*, L23202, doi:10.1029/2009GL041048.

Wilson, R. J., R. L. Tokar, M. G. Henderson, T. W. Hill, M. F. Thomsen, and D. H. Pontius Jr. (2008), Cassini plasma spectrometer thermal ion measurements in Saturn's inner magnetosphere, *J. Geophys. Res.*, *113*, A12218, doi:10.1029/2008JA013486.

Winglee, R. M., D. Snowden, and A. Kidder (2009), Modification of Titan's ion tail and the Kronian magnetosphere: Coupled magnetospheric simulations, *J. Geophys. Res.*, *114*, A05215, doi:10.1029/2008JA013343.

Young, D. T., et al. (2004), Cassini plasma spectrometer investigation, *Space Sci. Rev.*, *114*(1), 1–112, doi:10.1007/s11214-004-1406-4.

Young, D. T., et al. (2005), Composition and dynamics of plasma in Saturn's magnetosphere, *Science*, *307*, 1262–1266, doi:10.1126/science.1106151.

A. Kidder and R. Winglee, Department of Earth and Space Science, University of Washington, Box 351310, Seattle, WA 98195, USA. (ariah@u.washington.edu; winglee@ess.washington.edu)

D. Snowden, Lunar and Planetary Laboratory, University of Arizona, 1629 E. University Blvd., Tucson, AZ 85721, USA. (dsnowden@lpl.arizona.edu)